# Modeling of the ViscoLine Annular Heat Exchanger

Maria Navasa Guasch
Product Centre Compact Heat Exchangers, Alfa Laval, Lund
LTH, Lund University

February 2011

# Contents

# 1. Summary

The ViscoLine Annular heat exchanger (VLA) is a four annular concentric tube heat exchanger from Alfa Laval AB designed for processing mainly food products like purees. These type of fluids are highly viscous and known as non-Newtonian. The VLA unit is a commercialized product although there is lack of information of how does the heat exchanger work with precision and thus, only rough estimations based on experience can be done for simulating the VLA behavior.

In this project, a model of the VLA considering both heat transfer and pressure drops has been developed in order to obtain a reliable model of how the heat exchanger behaves when using non-Newtonian fluids so it can further be used for commercial purposes within Alfa Laval AB.

In parallel, tests on the VLA heat exchanger using the available fluids; water and oil which are Newtonian fluids, have been carried out to prove the validity of the elaborated code. These tests have been run in two different units. From an analysis on the results obtained from the code evaluation and a proper characterization of the non-Newtonian fluids, the behavior of these fluids in the VLA can be simulated. The results of this should conclude in a general correlation for the ViscoLine Annular heat exchanger when dealing with non-Newtonian fluids.

The model has been validated with regard to heat transfer. Pressure drop calculations agree with the measurements but there are issues that need to be followed closely: the singular pressure drop coefficients ($\xi$ factors), the wall viscosity effect and the pressure drop calculations in one of the units.

# 2. Preface

## 2.1. Origin of the Master Thesis

As a double degree student between ETSEIB (Escola Tècnica Superior d'Enginyeria Industrial de Barcelona) and LTH (Lunds Tekniska Högskola) within the TIME (Top Industrial Managers for Europe) program, the master thesis was the last step to become an engineer. Finding a master thesis that suited my interests, specially heat transfer, was at first a bit difficult due to the lack of knowledge of "how things work" in Sweden but thanks to Professor Stig Stenström and his contacts with Alfa Laval AB, things worked out and I could develop the present master thesis.

## 2.2. Motivation

In order to become a chemical engineer, in the last years I have taken many courses in different backgrounds. Despite the variety of subjects, my interests in heat transfer, energy efficiency as well as environmental concerns have been increasing with time mainly because the terms environment and efficiency are present almost everywhere in our nowadays society. Furthermore, the motivation of some teachers in these subjects has also influenced my interests as well as projects done regarding these fields within ETSEIB or LTH.

Moreover, a part from having special interest in heat transfer methods and theoretical concepts, real life applications are more interesting and amazing from my point of view. Heat transfer equipment as well as industrial facilities are matter of interest.

## 2.3. Previous requirements

In order to develop the present master thesis, knowledge in different backgrounds like heat transfer, rheology, mechanics or computer programming are needed.

Heat transfer in general requires knowledge in heat transfer methods as well as the basic concepts in this field. In order to understand how the heat exchanger works, one must know in which direction heat transfer takes place and how this heat is transfered, be able to calculate the amount of heat transfered in the unit, if there are heat losses or not, which is the efficiency of the heat exchanger, etc. For these

reasons, it is important to have some background in this field in order to develop the model as heat transfer is one of the main parts.

Moreover, some knowledge in rheology is also required especially regarding non-Newtonian fluids. It seems that one can just work with Newtonian fluids like water or oil but what happens in everyday life? Not everything is water and oil and different fluids with different behaviors must be treated. This leads to the necessity of knowing how these fluids can be mathematically modeled to deal with them and be able to calculate their properties as well as how they behave under different conditions. As an example, it is not the same to deal with water or with cement. In order to be able to work with cement, it is necessary to study its properties and behavior under different conditions so that one can obtain the maximum possible benefit from it.

It is required also to have previous knowledge in pressure drop calculations. Pressure drops are the other main subject in this model. One must be able to apply Bernoulli's equation in the system as well as know the difference between primary and singular pressure drops and how to calculate them. Pressure losses in heat exchangers as well in other equipment are very important. Directly related to the pressure drop concept are the friction factors. It is necessary to know the importance of the friction factors when calculating pressure drops as small variations in these values can give very different pressure drops. Moreover, it is necessary to know how friction factors can be calculated and which parameters they are dependent on.

Furthermore, computer programming skills are needed. In this master thesis, the use of Pascal language was required as one must work with Borland Delphi but previous knowledge of any other programming language is of great help.

From a general point of view, the knowledge acquired in all these fields is product of the work done, the continuous formation during the degree both in Lund and in Barcelona apart from the acquisition of the most practical matters during the development of the master thesis. All these skills have permitted to face the master thesis with the necessary tools counting always with the support from Alfa Laval and professors from LTH.

# 3. Introduction

## 3.1. Aims of the Master Thesis

The aim of this master thesis is to develop a model for the ViscoLine Annular heat exchanger (VLA) from Alfa Laval. The VLA unit is a four concentric tubular unit from Alfa Laval which is used for the heating, cooling and pasteurization of products with high viscosity or products that contain particulates like food [1]. This heat exchanger is currently in the sales market and is mainly distributed in India for manufacturing mango puree.

Although the heat exchanger is a commercialized product, a detailed model for the thermal and pressure drop behavior is needed and that is the main reason for developing this master thesis. Moreover, the thermal model obtained will be very useful for optimizing the heat exchanger and its applications as well as for further improvements.

From bibliography data, tests performed in the heat exchanger and programming skills, the model will be built. The main goal of this master thesis is the code that must be built so that this model can be introduced into Alfa Laval's program for designing thermal equipment.

## 3.2. Project scope

The development of a model for the ViscoLine Annular heat exchanger will allow to predict the behavior of the VLA in a more accurate manner than how is nowadays done. At present, rough estimations on the outgoing temperatures, heat loads and pressure drop calculations on the VLA are made with a code based on an Excel sheet and with the only feedback from the sold units. However, experimental data should be obtained in order to verify the calculated values from the current method. Knowledge on thermodynamics, rheology, experimental tests and the development of a mathematical model should result in a thermodel which should be used to predict the behavior of the VLA for different types of fluids in an accurate manner. It is important to develop a model that can be used with different kinds of fluids as from an economic point of view is more efficient and moreover, as the VLA is a heat exchanger intended to use in the food industry, small modifications in the model should be introduced in order to adapt the model to as many different types

of fluids as needed. Furthermore, the development of a computer code or program should facilitate all these calculations and applications.

The general methodology used to obtain the model can be applied to any other type of heat exchanger which presents some similarities to this heat exchanger. That is for example, difference in length, considering insulation of the outer tube, some special kind of insert or mixing facility, etc. For each heat exchanger to be studied, all singularities must be taken into account in order to obtain a precise model that describes properly the behavior of the equipment.

It is important to develop a good and reliable model to predict the VLA behavior as it will allow to obtain the maximum benefit of the unit and thus, higher performance of the heating/cooling process.

In conclusion, the model and the code developed can be used as tools that will allow to implement the Viscoline Annular Heat Exchanger in the food industry.

# 4. Background theory

The main goal of this chapter is to define some basic theoretical concepts in order to be able to understand the basis of the project.

## 4.1. Rheology

Rheology is the discipline of fluid mechanics that studies the relationship between the deformation of a fluid and stress.

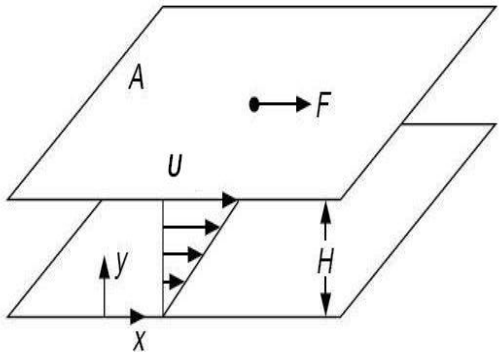


Figure 4.1: Deformation of a fluid under shear stress [2]

A fluid is a substance which undergoes continuous deformation when it is subjected to **shear stress** as shown in Figure 4.1. As it can be seen, a fluid is bounded between two large parallel plates of area $A$ separated by a distance $H$. The lower plate is fixed while the upper plate moves with a velocity $U$ due to the application of a force $F$ on the surface. The fluid continues deforming as long as the force is applied unlike a solid would do as it would only undergo a finite deformation. The force applied $F$ is directly proportional to the area $A$ of the plate which defines the shear stress ($\tau$) as:

$$\tau = \frac{F}{A} \tag{4.1}$$

As shown in Figure 4.1, a linear velocity profile within the fluid is established, $u = \frac{Uy}{H}$. In the lower plate, the boundary fluid's velocity is zero due to the no-slip

condition while in the upper plate, the fluid bounding the plate moves at the same velocity as the plate, $U$. So, the velocity gradient for this flow is known as the **shear rate** ($\dot{\gamma}$).

$$\dot{\gamma} = \frac{\partial u}{\partial y} \tag{4.2}$$

The ratio between the shear stress and the shear rate is the **viscosity**, the dynamic viscosity ($\mu$). The SI units of the dynamic viscosity are Pas or kg/ms.

$$\mu = \frac{\tau}{\dot{\gamma}} \tag{4.3}$$

Fluids can be classified into different rheological types in reference to the simple shear flow of Figure 4.1. In general, fluids can be classified as **purely viscous** or **viscoelastic fluids**. Purely viscous fluids are those which do not show any elastic behavior, that is when shear stress is removed, they do not undergo reverse deformation. The shear stress depends only on the rate of deformation. On the other hand, viscoelastic fluids are those which exhibit both elastic and viscous properties. Moreover, purely viscous fluids are classified into **time-independent** and **time-dependent** fluids. For **time-independent** fluids, the shear stress depends only on the instantaneous shear rate while for time-dependent fluids, the shear stress depends on the past history of the rate of deformation [2].

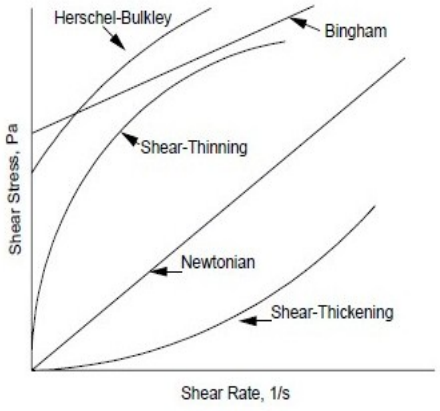


Figure 4.2: Rheograms for time-independent fluids [15]

The shear stress versus the shear rate for a fluid in simple shear rate can be plotted in a graph known as rheogram. Rheograms for several types of time-independent fluids are shown in Figure 4.2. The fluid rheogram which presents the highest engineering importance is the **Newtonian fluid** rheogram. From the figure it can be

seen that its rheogram is a straight line passing through the origin and the slope of this line is the viscosity. For a Newtonian fluid, the viscosity is independent of the shear rate and may be only temperature and perhaps pressure dependent. Then, Newton's law of viscosity, equation 4.4, is a rearrangement of equation 4.3. Typical Newtonian fluids are gases and low molecular weight liquids such as water.

$$\tau = \mu\dot{\gamma} = -\mu\frac{\partial u}{\partial y} \tag{4.4}$$

The other rheograms correspond to all those fluids whose viscosity varies with the shear rate or otherwise known as **non-Newtonian fluids**. For non-Newtonian fluids, the viscosity defined also as the ratio of shear stress to shear rate, is often called apparent viscosity to emphasize the difference from Newtonian behavior. Non-Newtonian fluids include also different kind of behaviors like for example the yield-stress materials. Yield stress materials are those for which a finite stress $\tau_y$ is required before continuous deformation occurs. The simplest yield-stress material is the **Bingham plastic** fluid. The constant slope that exhibits this fluid in the rheogram is called the infinite shear viscosity $\mu_\infty$, see the Bingham fluid equation.

$$\tau = \tau_y + \mu_\infty\dot{\gamma} \tag{4.5}$$

Another type of non-Newtonian fluids are the **shear-thinning fluids**. Shear-thinning fluids are those for which the viscosity decreases with increasing shear rate. Shear-thinning fluids are also known as pseudoplastics. Many polymer solutions as well as solid suspensions are shear-thinning. Shear-thinning fluids typically obey a power-law model, equation 4.6.

$$\tau = K\dot{\gamma}^n \tag{4.6}$$

Then, the apparent viscosity is defined as:

$$\mu = K\dot{\gamma}^{n-1} \tag{4.7}$$

Where:

$K$ is the consistency index or power law coefficient, $\left[\frac{\text{kg}}{\text{ms}^{2-\text{n}}}\right]$

$n$ is the power law index, dimensionless

For shear-thinning fluids, $n<1$.

The other non-Newtonian fluids are the **shear-thickening fluids**. Shear-thickening fluids are those whose viscosity increases with increasing shear rate. Shear-thickening fluids are also known as dilatant fluids and they may be described by the power law model, with $n>1$, by equation 4.6 for a limited range of shear rate. Shear-thickening

fluids are not very common, some particle solutions exhibit dilatancy at certain concentration ranges.

### 4.1.1. Fluid flow regimes

The flow regimes of a liquid or a gas can be laminar or turbulent. The flow regime of a fluid depends on the relationship between the inertia and viscosity forces (internal friction) in the stream [3]. This relationship can be expressed by a dimensionless group, the Reynolds number ($Re$):

$$Re = \frac{\rho u D_{\mathrm{h}}}{\mu} \tag{4.8}$$

Where:

$\rho$ is the fluid's density, $\left[\frac{\mathrm{kg}}{\mathrm{m}^3}\right]$

$u$ is the average velocity of the fluid, ratio between the volumetric flow and the cross-sectional area, $\left[\frac{\mathrm{m}}{\mathrm{s}}\right]$

$D_{\mathrm{h}}$ is the hydraulic diameter of the pipe or conduction, [m]

$\mu$ is the dynamic viscosity of the fluid, [Pas]

#### Laminar flow

Laminar flow occurs when a fluid flows in parallel stream layers without mixing with each other and flow smoothly past any obstacles encountered in their way. This means that the fluid's particles flow in parallel layers as mentioned before, there is no macroscopic mixture of the fluid and the only method of transport of energy, mass and momentum is the molecular transport. Laminar flow is characterized by a high diffusion and low convection momentums. Moreover, a laminar velocity profile has a parabolic shape where the maximum velocity is located at the center of the pipe and the velocity is zero at the pipe edges. Laminar flow is characteristic in low velocity fluids or in highly viscous fluids.

#### Turbulent flow

Turbulent flow is characterized by not having smooth streamlines and the velocity shows chaotic fluctuations due to random displacement of finite masses of the fluid which mix strongly with each other. The fluid's particles and macroscopic portions of the fluid (which circulate at a higher velocity) mix with each other randomly and moving in all directions. Then, there is a special contribution to the molecular transport which is dominant and is known as the turbulent transport [7].

Although the critical velocity at which the regime switches from laminar to turbulent may be different according to the fluid and the type of pipe, the Reynolds critical number is always the same, $Re_c = 2100$ for circular pipes. Generalizing:

$$Re < 2100 \text{ Laminar regime}$$
$$2100 < Re < 10000 \text{ Transition regime}$$
$$Re > 10000 \text{ Turbulent regime}$$

Sometimes, in the transition regime, the laminar regime can be metastable but any possible alteration turns it into turbulent. Moreover, the turbulent regime starts developing at low Reynolds numbers in the transition zone but it is not fully developed until it reaches $Re$=10000. In cylindric pipes, above $Re$=10000, laminar regime does not exist and below 2100 it is impossible to find turbulent flow [7].

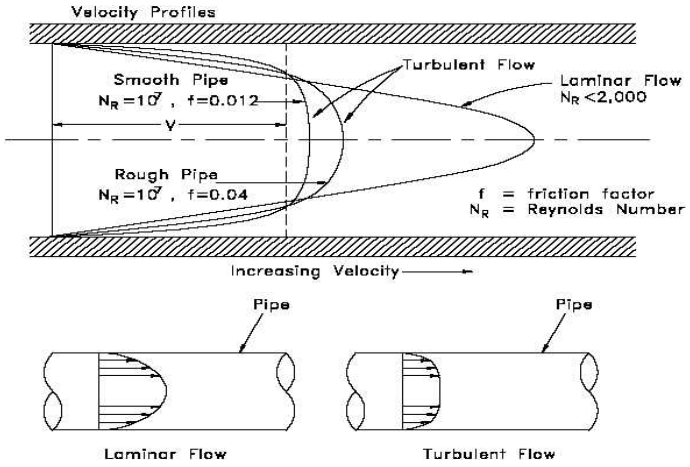


Figure 4.3: Laminar and turbulent flow velocity profiles [19]

## 4.2. Heat transfer

Heat transfer is the science that studies the energy transfer between two systems or inside a system due to a difference in temperatures. There are three fundamental types or modes of heat transfer: conduction, convection and radiation and all of them can take place at the same time [4].

### 4.2.1. Conduction

Conduction is considered as the energy transfer between the particles with higher energy to the particles with lowest energy of a substance due to the particle interaction. Conduction can take place through two mechanisms:

1. **Diffusion**: Molecules close to each other interact exchanging kinetic energy which means that energy diffuses from the hottest spots to the coldest ones. This mechanism depends on the molecular aggregation. With higher molecular aggregation, more important is this mechanism so, solids are better conductors than liquids and these, better than gases.

2. **By migration of free electrons**: When applying a thermal field to a material with metallic structure, the electrons migrate in the same way as they do when an electric field is applied which means that good electricity conductors are also good thermal conductors (aluminum, copper, etc.).

In a system where there is a specified temperature gradient, the energy flow transmitted as heat by conduction follows Fourier's law.

$$q_x = -\lambda A \frac{dT}{dx} \tag{4.9}$$

Where:

$\lambda$ is the thermal conductivity which is a characteristic from each substance. In general, $\lambda$ is function of temperature but for gases is also pressure dependent, $\left[\frac{\mathrm{W}}{\mathrm{mK}}\right]$

$A$ is the perpendicular area to the heat transfer direction, $[\mathrm{m}^2]$

$\frac{dT}{dx}$ is the temperature gradient in the x direction, $\left[\frac{\mathrm{K}}{\mathrm{m}}\right]$

### 4.2.2. Convection

Heat transfer by convection involves heat transport through one phase and the mixture of hot and cold portions of a gas or liquid. If the fluid movement is due exclusively to a density difference originated by temperature difference in the fluid, it is known as natural convection. However, if an external agitation influences the movement, then it is known as forced convection. In fluids, heat transfer by conduction is negligible against heat transfer by convection.

Heat transfer by convection of a fluid which is in contact with a hot surface follows Newton's law.

$$q_x = hA(T_\mathrm{s} - T_\mathrm{f}) \tag{4.10}$$

Where:

$h$ is the superficial heat transfer coefficient by convection, $\left[\frac{\mathrm{W}}{\mathrm{m^2K}}\right]$

$A$ is the perpendicular area to the heat transfer direction, $[\mathrm{m}^2]$

$T_\mathrm{s}$ is the surface temperature

$T_\mathrm{f}$ is the fluid temperature

### Heat transfer coefficient

The heat transfer coefficient ($h$) that appears in Newton's law, equation 4.10, is dependent on the system's geometry and the fluid's properties and velocity. It can be determined in three different ways [7]:

1. Experimentally, obtaining correlations whose general formula is deduced by dimensional analysis.

2. From the Boundary-layer Theory due to analysis and mathematical treatment of the hydrodynamic and thermal boundary-layer.

3. By analogy with other transport phenomena, specially, momentum transport.

Methods 2 and 3 can only be used in simple cases, specially if the regime is laminar. Method 3 can also be used for straight conduits under turbulent regime.
In the frequent case of heat transfer by convection in an internal turbulent flow, a liquid or a gas that circulates through a pipe in order to be heated or cooled from the outside, different empirical correlations exist based on a general relation deduced from dimensional analysis:

$$Nu = f(Re,Pr) \tag{4.11}$$

Where:
$Nu$ is the Nusselt number
$Re$ is the Reynolds number, equation 4.8
$Pr$ is the Prandtl number

Nusselt, Reynolds and Prandtl are non-dimensional numbers. The Reynolds number has been described previously but the Nusselt and the Prandtl numbers are defined as it follows:

$$Nu = \frac{hD}{k} \tag{4.12}$$

$$Pr = \frac{c_p \mu}{k} \tag{4.13}$$

Where:
$h$ is the superficial heat transfer coefficient by convection, $\left[\frac{\mathrm{W}}{\mathrm{m^2K}}\right]$
$D$ is the pipe's diameter, [m]
$\mu$ is the fluid's dynamic viscosity, [Pas]
$k$ is the fluid's thermal conductivity, $\left[\frac{\mathrm{W}}{\mathrm{mK}}\right]$
$C_p$ is the fluid's specific heat at constant pressure, $\left[\frac{\mathrm{J}}{\mathrm{kgK}}\right]$

The general correlation, equation 4.11, is valid for forced convection and fully developed flow. In case of natural convection, other forces are present, the buoyancy forces, and thus, another non-dimensional number is also used.

**Forced convection** Although there are many empirical correlations for internal flow that relate the heat transfer coefficient with the fluid and flow's variables, one must point out the very known Dittus–Boelter equation deduced for turbulent flow and cylindric smooth tubes [7]:

$$Nu = 0{,}023 Re^{0,8} Pr^{n} \tag{4.14}$$

Where:
$n = 0{,}4$ for a heating case
$n = 0{,}3$ for a cooling case

This equation is valid for fluids in which $0{,}6 < Pr < 100$, $Re > 10000$ and with moderate differences of temperature between the wall and the fluid. Fluids' properties are evaluated at the average temperature of the fluid [7].

**Natural convection** When heat transfer by natural convection takes place between a surface and the fluid that surrounds it, the most common empiric correlations for the heat transfer coefficient follow the form:

$$Nu = a(GrPr)^{m} \tag{4.15}$$

Where:
$Gr$ is the Grashof number
$Pr$ is the Prandtl number, equation 4.13
Constants $a$ and $m$ depend on the geometry and the position of the surface

The Grashof number is defined as it follows:

$$Gr = \frac{g\beta(T_0 - T_\infty)D^3}{\upsilon^2} \tag{4.16}$$

Where:
$g$ is the acceleration due to Earth's gravity, $[\frac{\mathrm{m}}{\mathrm{s}^2}]$
$\beta$ is the volumetric coefficient of expansion ($\beta = 1/T$, $T$ is the absolute temperature), $[\mathrm{K}^{-1}]$
$D$ is the pipe's diameter, [m]
$\upsilon$ is the kinematic viscosity of the fluid, $[\frac{\mathrm{m}^2}{\mathrm{s}}]$

### 4.2.3. Radiation

Every surface above the absolute zero of temperatures emits radiation. Due to the atomic vibration, a disruption of the electromagnetic field is generated (electromagnetic waves) which is more intense with higher temperature. Two surfaces at different temperature transfer heat if between them there is a transparent medium (diatomic gases) or vacuum. Heat is transfered from the hottest surface to the coldest and it

is transfered at the light velocity in the medium. This means that radiation is the fastest heat transfer mode. Moreover, only the radiant energy exchange between opaque bodies is considered. For this systems, the radiation is absorbed quickly at a short distance from the surface by interaction with matter [4].

A black body absorbs all the radiant energy that reaches it and emits the maximum possible energy as it is considered an ideal surface. This energy flow emitted by a black body at the absolute temperature $T$ (emissivity) is expressed by Stefan–Boltzmann's law.

$$E_b = \int_{\lambda=0}^{\infty} E_{b,\lambda} = \sigma T^4 \tag{4.17}$$

Where:
$\sigma = 5{,}67 \cdot 10^{-8} \left[\frac{\mathrm{W}}{\mathrm{m^2K^4}}\right]$, Stefan–Boltzman's constant

## 4.3. Pressure drop

Pressure drop is the concept associated to a pressure diminution of a fluid circulating through a pipe. Actually, the pressure drop is an energy loss by friction due to its viscosity which can be very important in Bernoulli's equation. In this section, Bernoulli's equation will be derived and the two existing types of pressure drops will be defined.

### 4.3.1. The Bernoulli Equation

The Bernoulli equation is the macroscopic version of the mechanical energy balance under the following assumptions [15]:

- Compression effects are negligible
- No thermal phenomena
- Non-viscous fluid
- The fluid is in steady state

The energy-work theorem expresses that the work all forces do is the same as the energy increase between sections 1 and 2.

$$W = W_{\text{int}} + W_{\text{ext}} = \Delta E \tag{4.18}$$

To be able to obtain Bernoulli's equation, both terms of the equality must be treated separately.

The left part of the equality corresponds to the work done by all the forces:
$W_{\text{int}}$ is the work due to internal forces. $W_{\text{int}} = 0$ because the fluid is incompressible

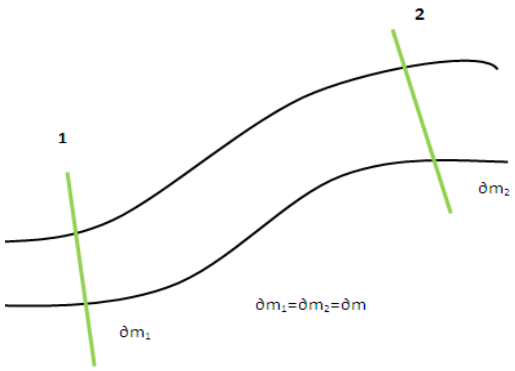


Figure 4.4: Sketch of sections 1 and 2 of an arbitrary pipe

and there are no viscous forces. $W_{\text{ext}}$ is the work due to external forces and as the fluid is non-viscous, the friction between the pipe and the liquid is not taken into account.

This leads to the following equation:

$$W_{\text{ext}} = p_1 A_1 u_1 dt - p_2 A_2 u_2 dt \tag{4.19}$$

The right term of the equality is related to the energy increase between sections 1 and 2 which can be expressed as:

$$\Delta E = \Delta U + \Delta E_{\text{M}} \tag{4.20}$$

$\Delta U$ is the internal energy variation. $\Delta U = 0$ because there are no compression works nor thermal phenomena. Moreover, the mechanical energy can be expressed as the sum of the kinetic and the potential energy as follows:

$$\Delta E = \Delta E_{\text{M}} = \Delta E_{\text{K}} + \Delta E_{\text{P}} = \frac{1}{2}\partial m(u_2^2 - u_1^2) + \partial m g(h_2 - h_1) \tag{4.21}$$

Where $h_1$ and $h_2$ are the heights of section 1 and 2 respect to an arbitrary level. However, it does not matter which is the reference as what it really matters is the relative height between both sections.
Replacing equation 4.19 and equation 4.21 into equation 4.18, that $A_i u_i dt = \frac{dm}{\rho_i}$ and that $\rho_1 = \rho_2 = \rho$, leads to the following expression:

$$p_1 + \frac{1}{2}\rho u_1^2 + \rho g h_1 = p_2 + \frac{1}{2}\rho u_2^2 + \rho g h_2 \tag{4.22}$$

However, as sections 1 and 2 are two arbitrary sections, one can express equation 4.22 as it follows. This equation is known as the Bernoulli equation for circular ducts.

$$\Delta p + K\left(\frac{1}{2}\rho u^2\right) + \rho g h = \text{Constant} \tag{4.23}$$

Where:
K=1 for turbulent flow
K=2 for laminar flow

This means that Bernoulli's equation expresses the energy conservation of an ideal fluid in an incompressible and steady flow. All the terms in the equation have energy per volume units. Moreover, from equation 4.23 it can be seen that the dynamic pressure is constant through an ideal flow. The dynamic pressure is the sum of the static pressure ($p + \rho g h$) and the kinematic pressure ($\frac{1}{2}\rho u^2$). Once the Bernoulli equation has been defined and understood, one can go into detail with the pressure drop concept. There are two types of pressure drops: primary and secondary.

Primary or continuous pressure drops are the pressure drops associated with the friction between the fluid and the wall pipes and the friction between fluid layers in laminar flow or between fluid particles in turbulent flow. They take place in uniform flow which means it usually happens in a constant section straight pipe. On the other hand, secondary or singular pressure drops take place when transitions, valves, turns, etc. are present. If the pipe is large and straight, secondary pressure drops are no matter of interest but, if the pipe is not really large and presents different elements such as the ones described previously, they can become very important and even be greater than the primary pressure drops. Furthermore, factors like pipe's roughness and laminar or turbulent flow have great impact when calculating pressure drops [15].

Considering a real life pipe system, between two arbitrary points, Bernoulli's equation (equation 4.22) with losses is verified.

$$p_1 + \frac{1}{2}\rho u_1^2 + \rho g h_1 = p_2 + \frac{1}{2}\rho u_2^2 + \rho g h_2 + \Delta P_{1-2} \tag{4.24}$$

Where the term $\Delta P_{1-2}$ is known as pressure drop and considers both primary and secondary pressure drops.

### 4.3.2. Primary Pressure Drops

In the middle of the $19^{th}$ century, experiments developed in a constant section water pipe showed that the pressure drop was directly proportional to the pipe length and to the square of the average fluid velocity and inversely proportional to the pipe's diameter. This behavior is expressed by Darcy–Weisbach's equation. This equation is the general equation for primary pressure drops in circular pipes which means it is valid for both laminar and turbulent flows [15].

$$\Delta P_{(1-2)\mathrm{p}} = \lambda \frac{L}{D} \frac{\rho u^2}{2} \tag{4.25}$$

Where:

$\lambda$ is the Darcy–Weisbach friction factor, dimensionless
$L$ is the pipe length, [m]
$D$ is the pipe's diameter, [m]
$u$ is the average velocity in the pipe, $\left[\frac{\mathrm{m}}{\mathrm{s}}\right]$
$\rho$ is the fluid's density, $\left[\frac{\mathrm{kg}}{\mathrm{m}^3}\right]$
$\Delta P_{(1-2)\mathrm{p}}$ is the primary pressure drop of the pipe, [Pa]

Darcy–Weisbach's equation is known also as Fanning's equation, which can also be used in a generalized way no matter which type of fluid regime is present. The difference between these two equations is that the Darcy–Weisbach's friction factor from equation 4.25 is substituted by the Fanning's friction factor, $f$:

$$\Delta P_{(1-2)\mathrm{p}} = 2f \frac{\rho u^2 L}{D} [\mathrm{Pa}] \tag{4.26}$$

Where:

$$\lambda = 4f \tag{4.27}$$

**Laminar flow** For laminar flow, the known Poiseuille equation is used. It expresses the pressure drop per unit length due to the friction of a fluid of viscosity $\mu$ that flows with an average velocity $u$ through a circular pipe of diameter $D$. Poiseuille's equation, equation 4.28, is easily obtained from a momentum balance in the cylindric pipe and considering the velocity ratio $\frac{u}{u_{max}} = 0{,}5$ although is only valid under the following conditions: Newtonian fluid and laminar, steady, non-compressible and fully developed flow [15].

$$\frac{\Delta P_{(1-2)p}}{L} = \frac{32 \mu u}{D^2} \left[\frac{\mathrm{Pa}}{\mathrm{m}}\right] \tag{4.28}$$

**Friction factors**

The friction factor is a dimensionless number used in fluid mechanics which depends on the Reynolds number and the geometry of the system or in other words, it depends on the fluid's properties, the fluid's velocity and the diameter and roughness of the pipe. This leads to different ways of calculating the friction factor according to what type of fluid regime one is dealing with and as mentioned before, the system's geometry. This means that a circular pipe has a different friction factor than an annular pipe, a squared section pipe or any other geometry type [2].

Different correlations, mathematical and graphical, exist to calculate the friction factor at different Reynold's number and for different geometry systems but, as one can imagine, there is not an expression for every single geometry type. Some correlations for laminar and turbulent flow are presented in this project as they are used for modeling the pressure drop.

**Moody's graphical correlation** Experimental data from different authors with different values of velocity, density, viscosity, pipe length, pipe diameter and roughness were plotted by Moody in a graph, resulting in different curves as seen in Figure 4.5.

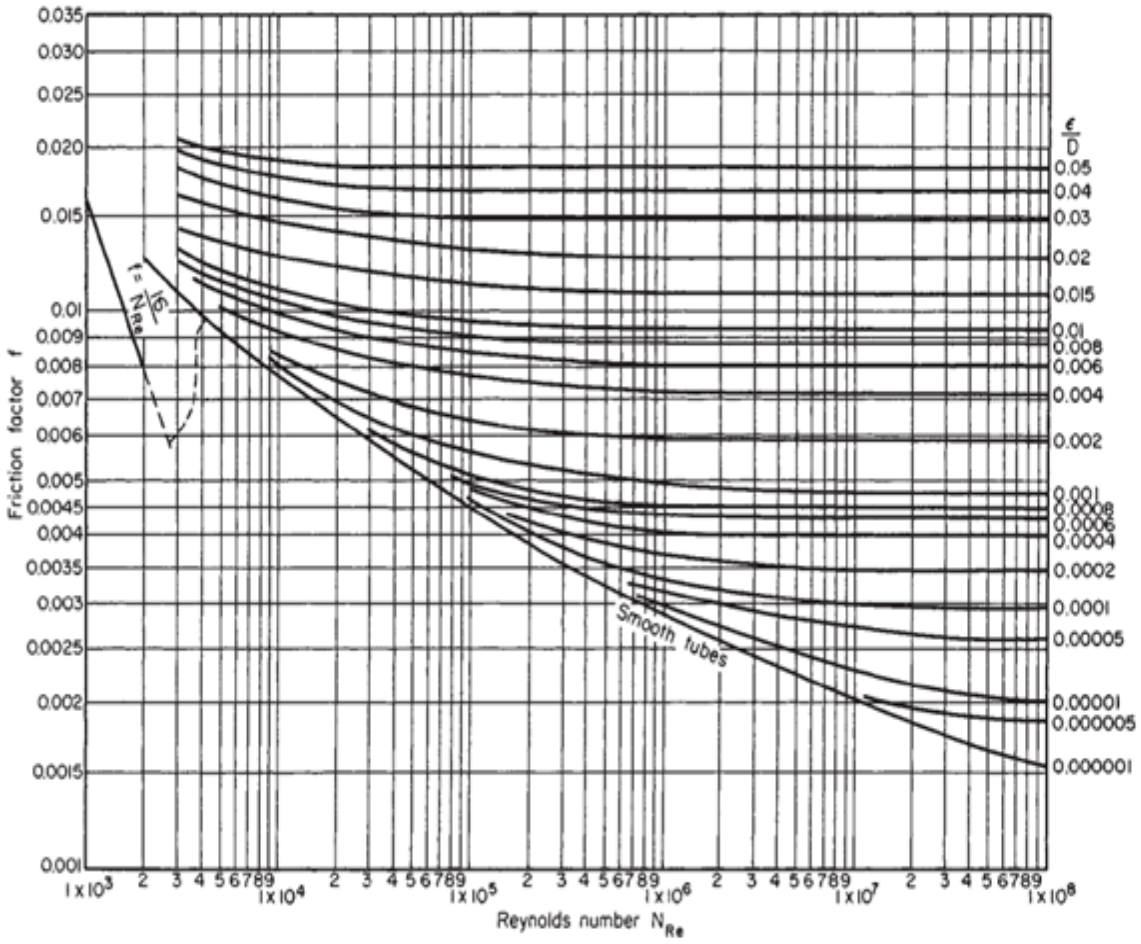


**FIG. 6-9** Fanning Friction Factors. Reynolds number Re = $DV\rho/\mu$, where $D$ = pipe diameter, $V$ = velocity, $\rho$ = fluid density, and $\mu$ = fluid viscosity. (*Based on Moody,* Trans. ASME, *66, 671 [1944].*)

Figure 4.5: Moody's chart from Perry's [2]

**Mathematical correlations** Different mathematical expressions exist for calculating the Fanning friction factor $f$, specially for turbulent flow. However, for the laminar regime, the friction factor expression is obtained from equation 4.28 and equation 4.26. The resulting expression is also plotted in Moody's chart, Figure 4.5.

$$f = \frac{16}{Re} \tag{4.29}$$

For turbulent flow, one of the most known and used correlation is the Colebrook–White formula:

$$\frac{1}{\sqrt{f}} = -2\log\left(\frac{\epsilon}{3{,}7D} + \frac{2{,}51}{Re\sqrt{f}}\right) \tag{4.30}$$

Where $\epsilon$ is the pipe roughness, [m].

All the previous equations have been deduced for circular pipes but when pipes are not circular, the hydraulic diameter concept can be used [7].

**Hydraulic diameter** Previous Fanning's friction equations where deduced for circular pipes but can also be used for cases in which the cross-sectional area is different like in air conditioning pipes (square or rectangular), concentric heat exchangers (annular cross-sectional area between the tubes), etc. For this reason, it is necessary to replace the circular diameter with the circular diameter of the non-circular pipe, which is defined as [7]:

$$D_\mathrm{h} = \frac{4A}{P_\mathrm{w}} \tag{4.31}$$

Where:

$A$ is the cross-sectional area of the flow, [m$^2$]

$P_\mathrm{w}$ is the wetted perimeter, [m]

For an annular cross-sectional area, the hydraulic diameter ($D_\mathrm{h}$) can easily be deduced from equation 4.31 leading to the following expression:

$$D_\mathrm{h} = D_\mathrm{out} - D_\mathrm{in} \tag{4.32}$$

Where:

$D_\mathrm{out}$ is the inner diameter of the outer tube, [m]

$D_\mathrm{in}$ is the outer diameter of the inner tube, [m]

However, different names are given to equation 4.31. For example, according to Perry [2] and Byron, Stewart and Lightfoot [6], the hydraulic diameter is defined as equation 4.31, four times the cross-sectional area divided by the wetted perimeter. While according to McCabe, Smith and Harriot [8] and Calleja et al. [7], this definition corresponds to the equivalent diameter. Moreover, while ones differentiate

between these two diameters, others do not which turns into confusion.

In this project, the first definition has been used, that is that the $D_{\mathrm{h}} = \frac{4A}{P_{\mathrm{w}}} = D_{\mathrm{out}} - D_{\mathrm{in}}$.

### 4.3.3. Singular Pressure Drops

Singular pressure drops are those produced by any type of object that placed in a pipeline, produces a major or minor obstruction to flow circulation. For example: valves, bends, section changes, way in and way out of the pipe, etc. As mentioned before, depending on the unit's geometry, singular pressure drops can be larger than primary pressure drops. For example, when valves are closed. Singular pressure drops can be calculated by two different methods. The first method is the easiest one and thus, the most used.
To estimate the singular pressure drops, the following expression is usually used:

$$\Delta P_{(1-2)\mathrm{s}} = \xi \rho \frac{u^2}{2} \tag{4.33}$$

Where $\Delta P_{(1-2)\mathrm{s}}$ is the singular pressure drop which is considered to be proportional to the average kinetic energy of the fluid. $\xi$ is the singular pressure drop coefficient which is non-dimensional and depends on the singularity (the geometry), the pipe's roughness and the average pipe velocity. $u$ is the fluid's velocity at the smallest cross-sectional area.

**The equivalent length method** However, the singular pressure drop can also be calculated using Fanning's equation when the flow is very turbulent by using the equivalent length concept ($L_{\mathrm{e}}$). This method consists of considering the singular pressure drop as an additional equivalent pipe length. The equivalent length is related to the singular pressure drop coefficient as it follows:

$$L_{\mathrm{e}} = \xi \frac{D}{f} \tag{4.34}$$

# 5. The VLA

## 5.1. Characteristics

The ViscoLine Annular heat exchanger or VLA is a tube-in-tube-in-tube-in-tube (four tubes) concentric heat exchanger in U-shape.

In order to be able to differentiate all the tubes, names will be defined and used further on in this text. The outermost tube (or tube 1) contains the utility medium as well as the inner tube (tube 3) and the central or innermost tube (tube 4). The product medium (tube 2) flows between the outermost tube and the inner tube in a counter-current mode. Moreover, the utility medium also flows in counter-current mode with the inner tube as it can be seen in Figure 5.1. *Leg 1* and *Leg 2* are the lengths that limit the U-turn.

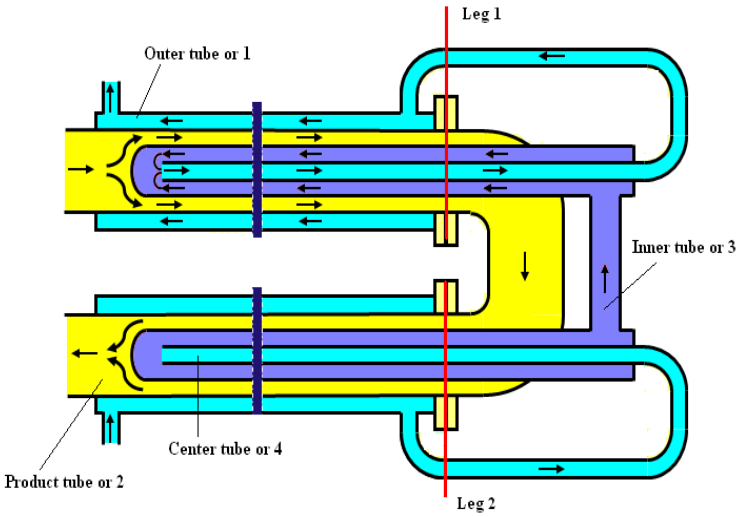


Figure 5.1: Flow principle in the VLA

The ViscoLine Annular Heat Exchanger comprises of different units that differ in size. There are basically two lengths (3 or 6 meters) and different tube diameter combinations as well as the possibility of having some static mixers on the product side to ensure a good mixture. ViscoLine Annular modules are usually connected in

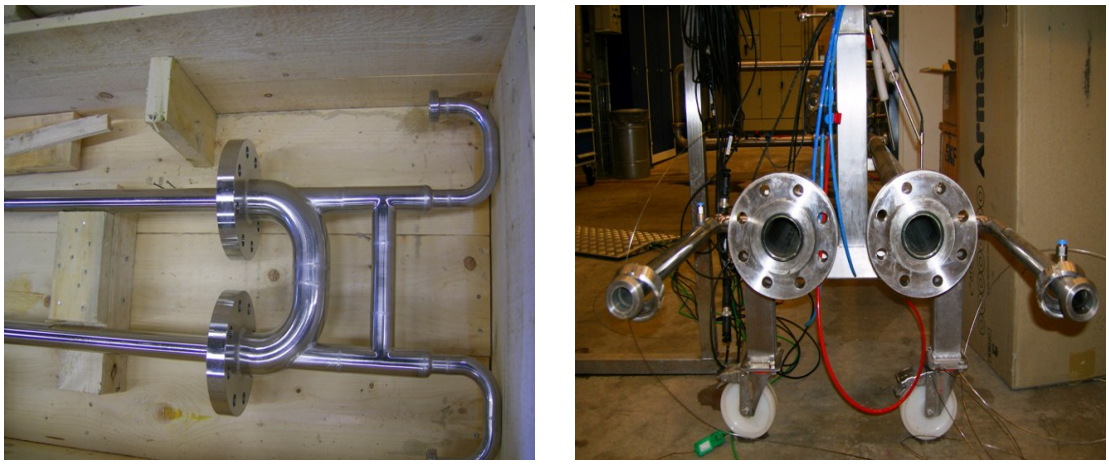

(a) A VLA insert (b) Union section of the insert with the unit

Figure 5.2: VLA's images taken at Alfa Laval's Thermal Products Test Center

series and grouped on a common frame in order to supply enough heat transfer to an industrial process. For specific data, consult the VLA brochure [1].

## 5.2. Tests

An important part of this master thesis consisted of testing the VLA in order to obtain real values that describe its behavior. The data obtained will be used to evaluate the code made.

### 5.2.1. Test Design

To prove the validity of the code developed for the VLA, tests on this unit were performed. This tests were possible thanks to Martin Johansson for supplying the unit and the different inserts that had to be tested and Anders Dahl and Milos Milovancevic for their work at Alfa Laval's Thermal Products Test Center.

As mentioned before, a VLA comprises of different units that differ mainly in its size. Due to its geometry and assembly, it is possible to change the center and the inner tubes for a certain unit giving different combinations. From now on, the different center and inner tubes combinations will be referred to as inserts. The tests were performed in a three meter length unit with three different types of inserts. Two of these inserts differ in the product gap size (insert 11 and insert 14) and the other one, contains static mixers (insert 11 with mixers). Insert 11 has 9,8 mm of product gap and item 14 has 15,8 mm. In Figure 5.2 (a), one can see an image of a VLA insert which comprises tubes 3 and 4 (inner and center tubes). In Figure 5.2 (b), the product tube can be seen and thus, the union place of the insert with the unit.

Table 5.1: Tests performed with their volumetric flow range (F) in $\left[\frac{m^3}{h}\right]$

| **Unit/Fluid** | | **Heat Transfer and Pressure Drops** | |
|---|---|---|---|
| p: product<br>u: utility | | *Heating* | *Cooling* |
| Item 11 | p: water<br>u: water | | $F_p = [0{,}9 - 14{,}4]$<br>$F_u = [0{,}9 - 6{,}5]$ |
| Item 11 | p: oil<br>u: water | $F_p = [0{,}5 - 9{,}0]$<br>$F_u = [0{,}5 - 5{,}9]$ | $F_p = [0{,}3 - 5{,}3]$<br>$F_u = [1{,}2 - 4{,}0]$ |
| Item 14 | p: water<br>u: water | | $F_p = [3{,}5 - 28{,}9]$<br>$F_u = [1{,}2 - 2{,}1]$ |
| Item 14 | p: oil<br>u: water | $F_p = [0{,}7 - 12{,}0]$<br>$F_u = [0{,}01 - 1{,}3]$ | $F_p = [0{,}8 - 6{,}3]$<br>$F_u = [1{,}2 - 1{,}2]$ |
| Item 11 MIXERS | p: water<br>u: water | | $F_p = [0{,}9 - 10{,}8]$<br>$F_u = [0{,}9 - 6{,}7]$ |

Previous to testing the unit, a design of how the tests should be performed was done. Temperature and pressure drops as well as flow rates were the elected parameters to be obtained from the experimental tests run at Alfa Laval's Laboratory. In Table 5.1 the tests run are indicated with the corresponding product and utility volumetric flow rates expressed in $m^3/h$. Pressure drops and temperatures were measured at the same time although they will be treated further on in this text by separate.

A decision about which were the necessary points and the place to measure these parameters had to be made. The flows are only measured at the exits of the heat exchanger but the temperature and the pressure drop are measured along the unit. In order to decide which were the optimal points for measuring the temperature, a temperature profile of the heat exchanger for a cooling and for a heating case was drawn, see Figure 5.3. See Figure 5.1 for locating *Leg 1* and *Leg 2* in the heat exchanger.

As it can be seen in both temperature profiles, in order to be able to have an accurate heat transfer model inside the VLA, the temperature must be measured in the following points (see Figure 5.3): the product inlet and outlet temperatures as well as the temperature in some point in the middle of the heat exchanger, the outer utility inlet and outlet temperatures, as well as the temperature where the center utility gets in contact with the inner utility. Moreover, the temperature of the inner utility at the U-turn and the center utility temperatures at the loops are matter of interest.

To measure the temperature, RTDs (Resistance Temperature Device) Pt100 (Pentronics Class A series 7504000) were used. In order to measure the temperature at the points where the inner and the center utility meet, special thermocouples were required (Pentronic, model 8102000, type K). The pressure drops are measured taking

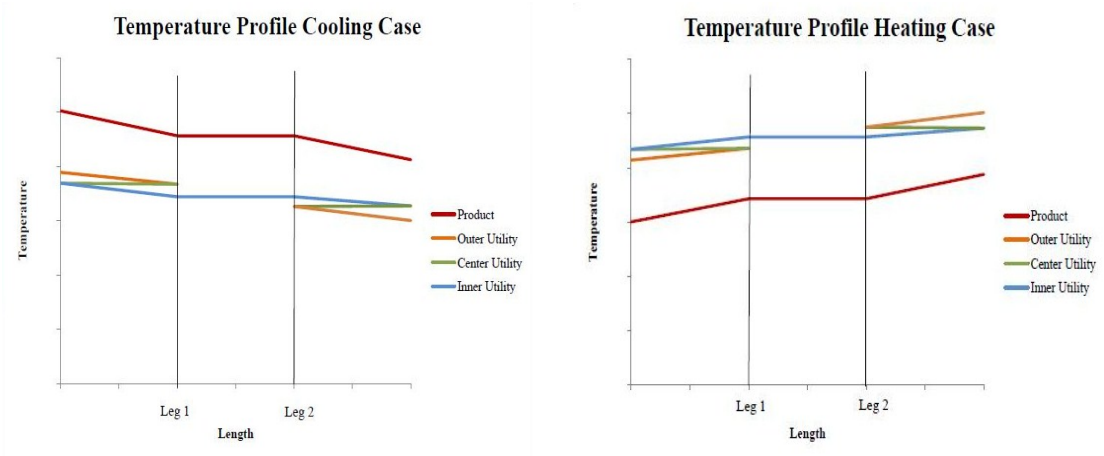


(a) Cooling Case (b) Heating Case

Figure 5.3: Temperature profiles for the VLA

as a reference the inlet product pressure for the product side and the inlet utility pressure for the utility side by using pressure transmitters (SattControl ETP-04, Rosemount 1151DP, SattControl ETD-04 and DRUCK DPI-705 which is a hand-held digital pressure indicator). Water flow rates are measured with magnetic flow meters (Fischer & Porter 10DX3112 and Fischer & Porter 10D 1465B with Process Data PD340 as the flow transmitter). Oil flow rates are measured with mechanical volumetric flow meters fitted with impulse transmitters ("BR" OaP2Ag19E/D2 and "BR" OaP50Ag19ED0). All transmitters, except the special thermocouples, are part of the regular calibration routines used in the laboratory which follow EN ISO/IEC 17025 "General requirements for competence of testing and calibration laboratories". The special thermocouples were calibrated separately. In Figure 5.4 (a), the points marked in red are the spots where the temperatures and pressures are measured in the heat exchanger. The pressure drop points for the utility side are numerated as the pressure drop between different points can be measured, which pressure drop is measured is specified in the Excel file that goes with the results. $AL\_PT100\_1$, $AL\_TC\_1$ and the others shown in the figure refer to the device used for measuring the temperature in the different points and thus, are the names found in the result sheet. In Figure 5.4 (b), the weldings for the temperature and pressure drop measuring devices are shown. Note the angle of the temperature inserts towards the flow direction.

Furthermore, as these tests are required for validating the model developed, they must cover the Reynolds range at which the heat exchanger is used in order to be as close as possible to a real situation. As said before, the VLA is a heat exchanger which deals with non-Newtonian fluids in the product side, specially food purees. As it was impossible to test with food due to fluid stability, availability and other reasons, instead oil was used although oil is a Newtonian fluid. As non-Newtonian fluids present low Reynolds numbers, the velocity required for the oil is very low

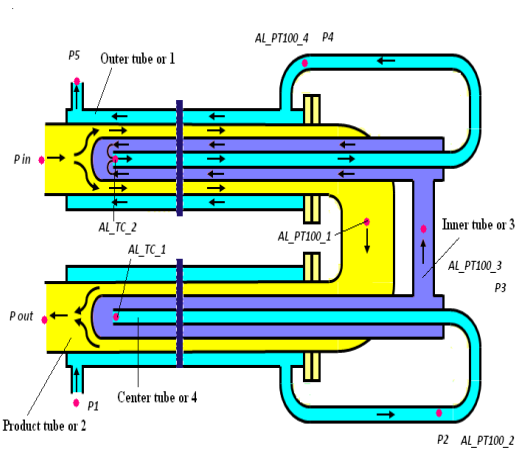


(a) Points in the VLA where temperature is measured

(b) A VLA unit, image taken at Alfa Laval's Thermal Products Test Center

Figure 5.4: The ViscoLine Annular Heat Exchanger

and this is taken into account in order to decide at which flows the temperatures and pressure drops must be measured, see Table 5.1. The oil used in the tests is Mobil DTE-3.

To sum up, three different inserts, a range of Reynolds numbers to cover and temperatures and pressure drops to measure. To obtain reliable values for the heat exchanger behavior, three different runs for each insert should be done. One considering the product flow as constant, another considering the utility flow as constant and the third one considering that both flows change. Moreover, for each insert, there will be a water/water case and a water/oil case. As it can be seen, there are many different combinations. However, tests are limited by the Test Center facilities and the fluids itself specially, when using oil as product which means that not all runs are possible.

### 5.2.2. Test Procedure

The performance test procedure used for testing the VLA is the test procedure that is used at Alfa Laval's Thermal Products Test Center [17]. This procedure follows the European Standards EN 305 "Heat Exchangers: Definitions of performance of heat exchangers and the general test procedure for establishing performance of all heat exchangers" and EN 306 "Heat Exchangers: Methods of measuring the parameters necessary for establishing the performance".

The procedure basically describes which are the necessary parameters to be measured as well as the necessary measuring equipment which for the VLA have been described previously. Moreover, the test procedure is described which basically con-

sists of connecting the heat exchanger to the test rig with the test fluids, set the desired parameters and wait until steady-state is achieved to carry out the measurements (stabilized parameters, stabilized heat exchanger with the surroundings and completed inherent heating or cooling of the unit and the peripheral equipment) [17].

The desired parameters (temperature, pressure drops, flow rates and valves) are set and controlled automatically. In Figure 5.5 an image of the screen where the parameters can be controlled is shown. For each test, a different rig has been used. However, they have the same arrangement but what differs is the fluids. For the water/water test rig, see Figure 5.6, and for the oil/water tests rig, see Figure 5.7.

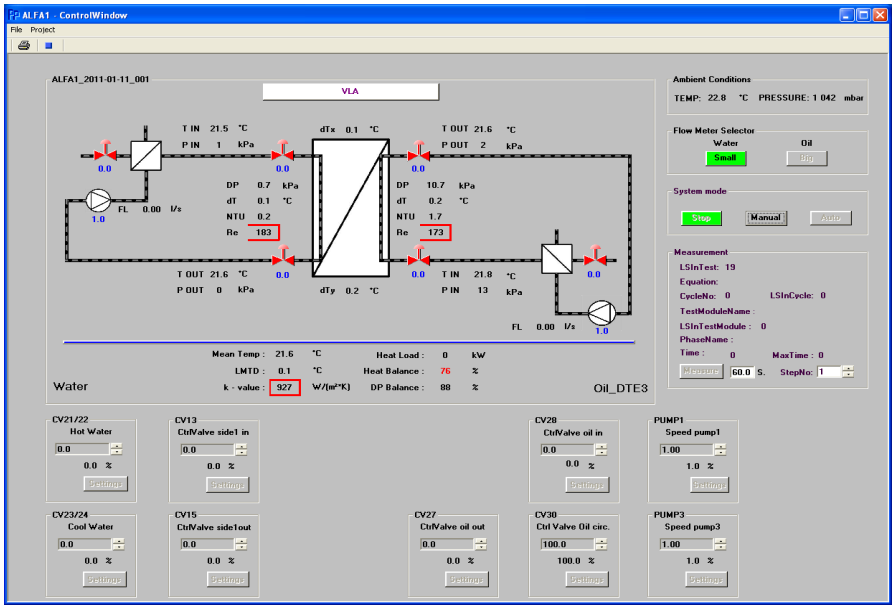


Figure 5.5: Image of the program screen for the laboratory test performances from Alfa Laval's Thermal Products Test Center

The tests results are property of Alfa Laval AB.

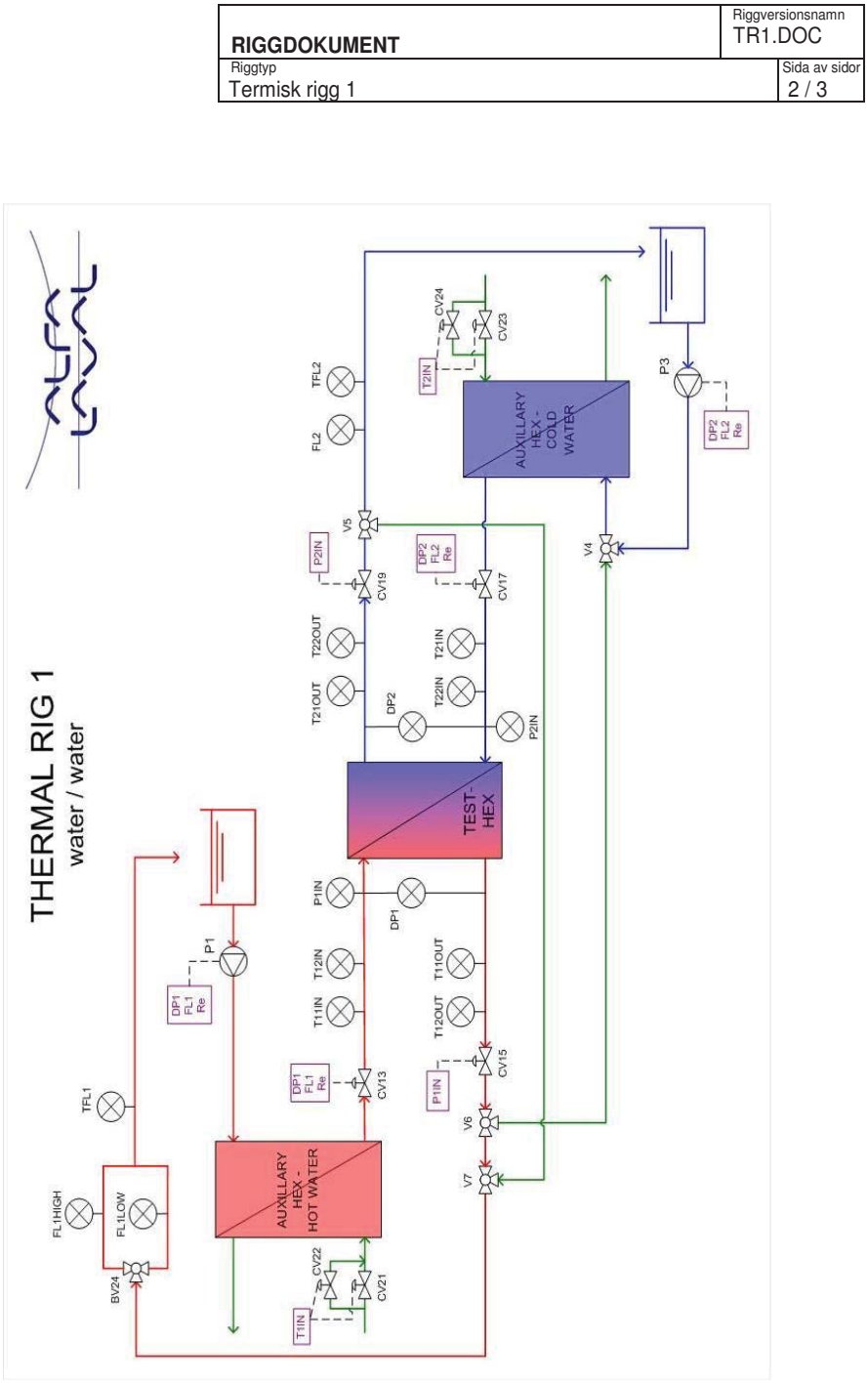


Figure 5.6: Water/water test rig from Alfa Laval's Thermal Products Test Center

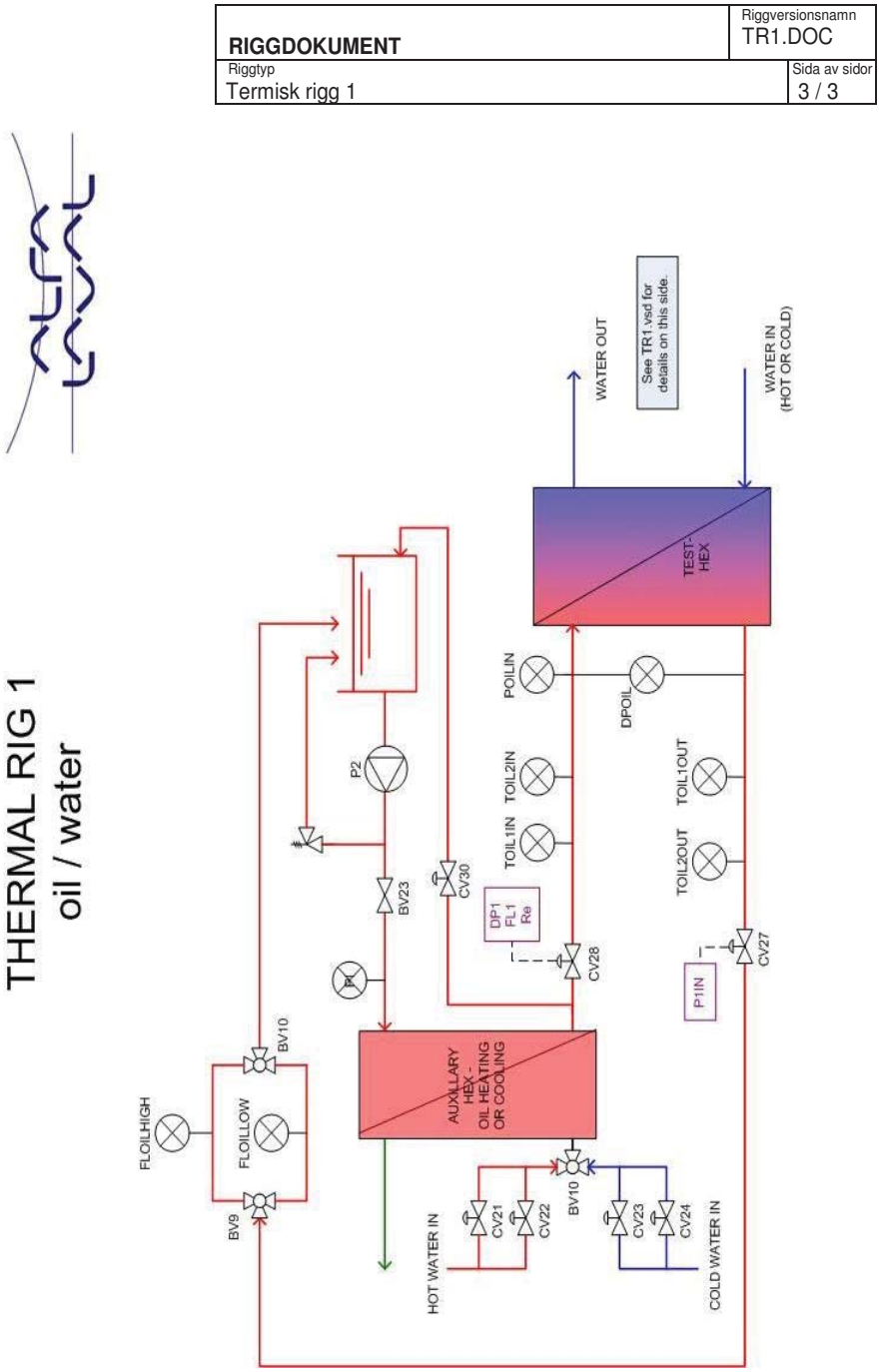


Figure 5.7: Oil/water test rig from Alfa Laval's Thermal Products Test Center

# 6. The Code

One of the goals of this master thesis is to develop a code in Pascal language using Borland Delphi for Alfa Laval in order to be able to simulate the behavior of the VLA and thus be further used in Alfa Laval's development of correlations for use in the sales organization. This code must consider heat transfer as well as pressure drop inside the unit.

The code, written in the Pascal language, must perform heat balances and pressure drops calculations through the whole unit to be able to describe its behavior. To do so, it was chosen to discretize the unit by dividing the heat exchanger into different elements. The element length is defined by the user and the smaller the size, more elements and thus, the more accurate are the calculations. However, the number of elements must be a compromise between accuracy and calculation time. The need of discretizing the unit is mainly to follow closely what happens along the whole heat exchanger and to be able to iterate in the whole unit.

## 6.1. Heat Transfer

The VLA is a 4 tube-in-tube heat exchanger which presents heat exchange in the radial direction as well as in the longitudinal direction. To be able to calculate the heat transfer in the whole unit, heat balances for each tube and for each element must be performed. Moreover, the VLA is a counter-current flow heat exchanger. This means that if the outgoing temperatures are to be known and calculations are done taking one side as reference, one temperature will be unknown. This implies the guessing or initialization of some values and thus, an iteration loop in order to converge them.

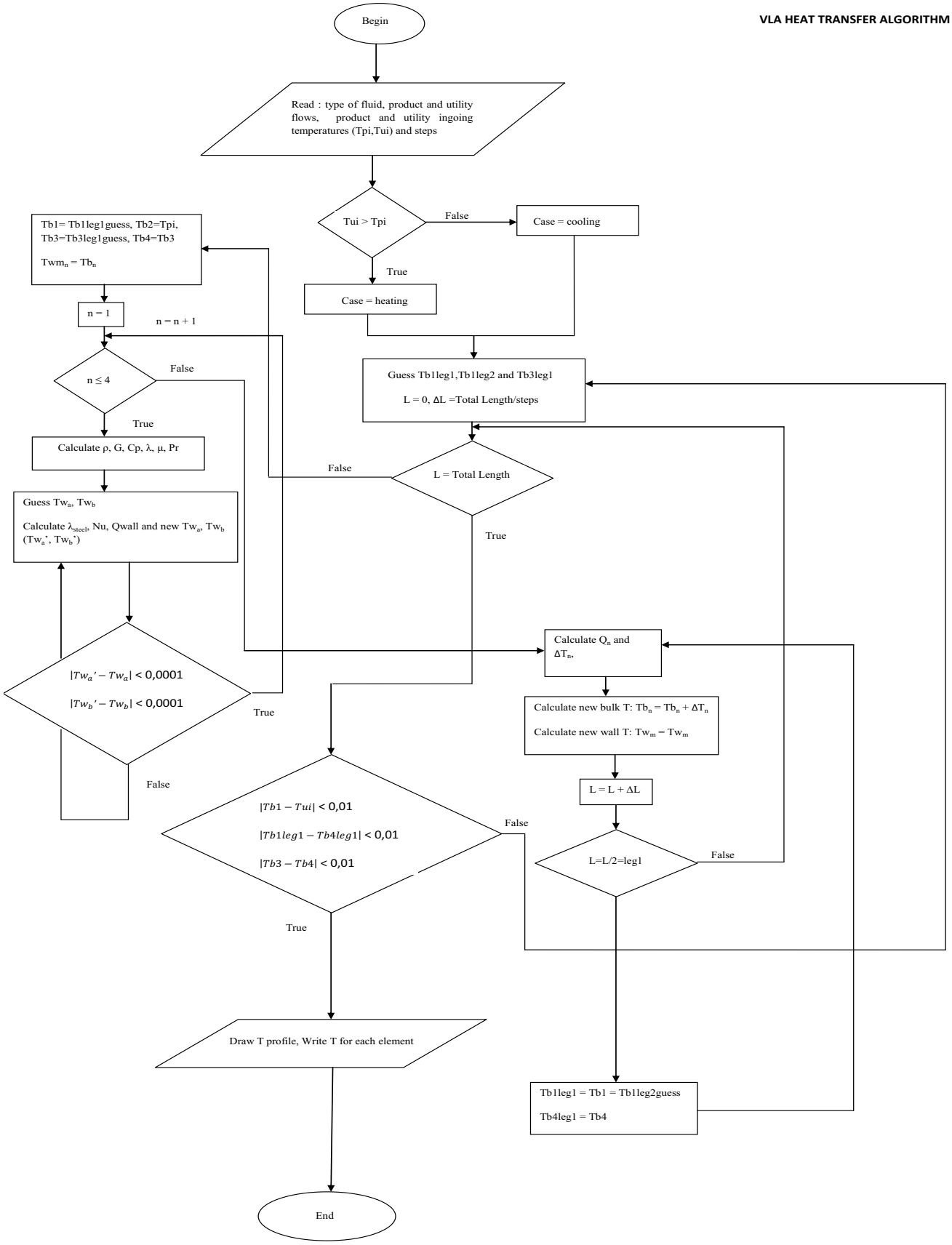


Figure 6.1: VLA's Heat Algorithm

Heat transfer calculations for the VLA are based on heat balances in the different tubes that form the exchanger. Only forced convection is considered as conduction is negligible when convection is present and no radiation effects are taken into account. The product ingoing side is set as a reference which means that the product ingoing temperature is known but not the outgoing utility temperature. Thus, the outgoing utility temperature must be initialized in order to perform all the necessary heat balances for each element in the heat exchanger. In Figure 6.1 the algorithm used for calculating the heat transfer in the VLA is shown. As it can be seen, first, the program must read which type of fluid one is handling (water, oil or a non-Newtonian fluid), the product and the utility flows ($G_i$), the product ingoing temperature ($T_{\text{pi}}$), the outer utility (tube 1) ingoing temperature ($T_{\text{ui}}$) and the number of steps which is the number of elements into which the exchanger is being discretized. Once these input data are read, calculations begin. First of all, it identifies if it is a cooling or a heating case. This step is mainly necessary for better temperature guesses when iterating. After the case identification, initialization of *Tb1leg1*, *Tb1leg2* and *Tb3leg1* is done. *Tb1leg1* is the bulk temperature of tube 1 or outer utility tube in *Leg 1*, *Tb1leg2* is the bulk temperature of tube 1 in *Leg 2* and so on. For better understanding of these temperatures, see Figure 6.2. Furthermore, the element length ($\Delta L$) is calculated according to the number of steps defined as an input.

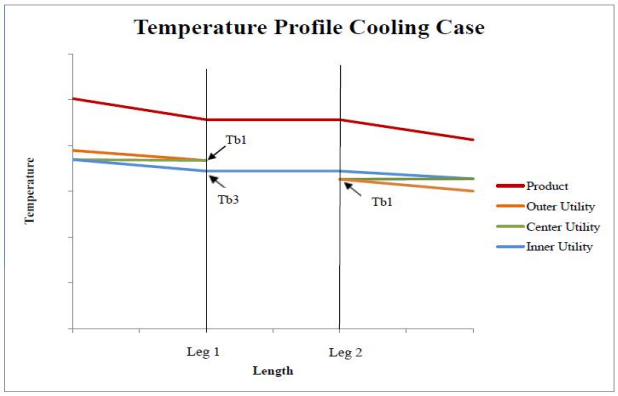


Figure 6.2: Temperature profile of the VLA for a cooling case

Once the elements' length are defined, calculations begin for the first element. For the first element, the utility bulk temperatures must be guessed as the only known temperature is the ingoing product temperature or $T_{\text{pi}}$. Next, for each tube ($n$), heat balances at their walls are performed. To do so, the wall temperatures must also be initialized. For each tube, fluid properties which depend on temperature like the density, the dynamic viscosity, the thermal conductivity, the specific heat at constant pressure ($Cp$) and the Prandtl number ($Pr$) are calculated. After the

physical properties are known, wall temperatures at each tube wall must be guessed so that the thermal conductivity of steel, the tubes' material, fluids' viscosities at wall temperatures and the heat transfer through the tubes' walls can be calculated. Looking into Figure 6.3, $T_{w1}$ and $T_{w2}$ are the wall temperatures of tube 1 which one must initialize. This must be done for the four tubes of the VLA as well as calculating the Nusselt number and the heat transfer coefficients by convection ($h$).

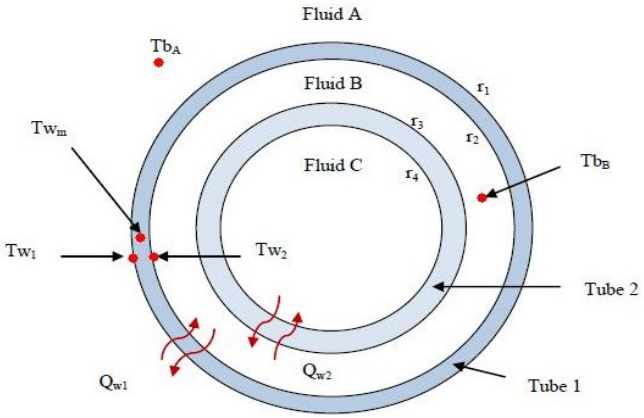


Figure 6.3: Sketch of a concentric annular pipe

The Nusselt number can be calculated through different correlations that the user can select from the created interface. The available Nusselt correlations depend on the type of flow regime which means that there are some correlations for laminar flow and some for turbulent flow. However, geometry also influences the Nusselt correlations which in reality means that it is easy to find correlations for circular pipes but difficulty increases when dealing with annular pipes and when using other types of fluids than water. In this project, the hydraulic diameter of an annular cross-sectional area has been used instead of a circular pipe's diameter when using Nusselt correlations for circular pipes. Different expressions for laminar and turbulent flow were obtained from the literature research.

For laminar flow, the Nusselt correlations are the following [16]:

- Sieder–Tate

$$\overline{Nu} = 1{,}86 \left(\frac{RePr}{(L/D)}\right)^{\frac{1}{3}} \left(\frac{\mu}{\mu_w}\right)^{0{,}14} \tag{6.1}$$

  Valid for $13 < Re < 2300; 0{,}48 < Pr < 16700; 0{,}0044 < \left(\frac{\mu}{\mu_w}\right) < 9{,}75$. $\mu$ is the viscosity at bulk temperature and $\mu_w$ is the viscosity at wall temperature.

- Hausen

$$\overline{Nu} = 3{,}66 + \frac{0{,}0668 PrRe(D/L)}{1 + 0{,}04\left[PrRe(D/L)\right]^{\frac{2}{3}}} \tag{6.2}$$

Valid for $13 < Re < 2300$ and completely developed flow.

- Stephan

$$\overline{Nu} = \left[3{,}66 + \frac{0{,}0677\left(PrRe\frac{D}{l}\right)^{1{,}33}}{1 + 0{,}1Pr\left(Re\frac{D}{L}\right)}\right]\left(\frac{\mu}{\mu_{\mathrm{w}}}\right)^{0{,}14} \tag{6.3}$$

Valid for $13 < Re < 2300; 0{,}48 < Pr < 16700; 0{,}0044 < \left(\frac{\mu}{\mu_{\mathrm{w}}}\right) < 9{,}75$. $\mu$ is the viscosity at bulk temperature and $\mu_{\mathrm{w}}$ is the viscosity at wall temperature.

All three equations are defined for a circular cross-sectional pipe.

If the velocity profile at the pipe's entrance is flat, a certain tube length is required in order to obtain a fully developed flow, see Hausen's equation. The necessary length to obtain a fully developed flow is known as the entrance length. For the laminar regime, at the pipe entrance, the velocity profile is flat and thus, the velocity is the same for all positions. As the fluid moves along the tube, the thickness of the boundary layer increases until both layers meet at the center of the pipe and the velocity profile is fully developed, see Figure 6.4.

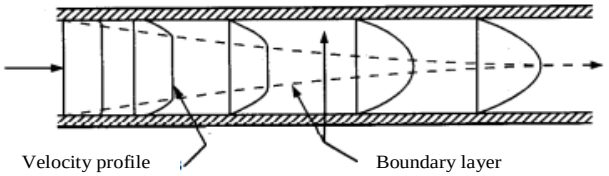


Figure 6.4: Velocity profile at a pipe's entrance for laminar flow

The approximated entrance length $L_{\mathrm{e}}$ of a pipe with diameter $D$ to achieve a fully developed laminar flow is [15]:

$$\frac{L_{\mathrm{e}}}{D} = 0{,}0575Re \tag{6.4}$$

The same happens with the temperatures. The approximated entrance length $L_{\mathrm{e}T}$ of a pipe with diameter $D$ to achieve a fully developed temperature profile is [15]:

$$\frac{L_{\mathrm{e}T}}{D} = 0{,}0575RePr \tag{6.5}$$

The previous Nusselt number equations are valid for completely developed flow. To verify that these equations can be used, the hydrodynamic entrance length calculated for a 20 mm diameter pipe with Re=10 is approximately 1 cm which is really

small compared to the 6 m total length of the heat exchanger. Thus, for laminar flow, the velocity profile is fully developed at the heat exchanger's entrance. Moreover, the temperature entrance length should be bigger than the hydrodynamic and thus, by dividing equation 6.5 into equation 6.4, the Pr number is obtained which from the data is around 900 verifying that indeed $L_{eT} >> L_e$.

For turbulent flow, $Re > 10000$, the Nusselt correlations are the following :

- Dittus–Boelter: circular duct, equation 4.14
- Monrad and Pelton: annular duct [2]

$$Nu = 0{,}020 Re^{0,8} Pr^{\frac{1}{3}} \left(\frac{D_{\text{out}}}{D_{\text{in}}}\right)^{0,53} \tag{6.6}$$

  Where $D_{\text{out}}$ is the inner diameter of the outer tube and $D_{\text{in}}$ is the outer diameter of the inner tube [m].

After the heat transfer coefficients have been calculated, the heat transfer between each tube wall must be calculated. According to Figure 6.3, the heat balance for one tube, for example tube 1, will be $Q_{\text{w1}}$ and taking into account the wall resistance for cylindrical geometry, one can express the heat balance for a tube or pipe in the following way:

$$Q_{\text{w1}} = \frac{T_{\text{b}A} - T_{\text{b}B}}{\frac{1}{2\pi h_A r_1 \Delta L} + \frac{\ln\left(\frac{r_1}{r_2}\right)}{2\pi\lambda_1 \Delta L} + \frac{1}{2\pi h_B r_2 \Delta L}} \tag{6.7}$$

Where:

$T_{\text{b}A}$ and $T_{\text{b}B}$ are the bulk temperatures of fluid A and B respectively

$h_A$ and $h_B$ are the superficial heat transfer coefficients by convection for fluid A and B respectively, $\left[\frac{\text{W}}{\text{m}^2\text{K}}\right]$

$\Delta L$ is the element length,[m]

$r_1$ and $r_2$ are the outer and inner radius of tube 1, [m]

Of course, $Q_{\text{w1}}$ can be positive or negative depending on the heat transfer direction, that is, how the temperature gradient is defined. Once the heat transfer at the wall is calculated, the new wall temperatures can be obtained if a heat balance between the bulk temperature of the fluid and the wall temperature close to that fluid is established, see equation 6.8. Then, the new bulk temperatures are compared to the old ones, the ones guessed, and if they are close enough, tolerance is set to be 0,0001 K, then the new wall temperatures are valid and calculations can move forward. However, if the difference between the new and the old temperatures is higher than the established tolerance, iterations must be done until they converge.

$$Q_{\text{w1}} = \frac{T_{\text{b}A} - T_{\text{w1}}}{\frac{1}{2\pi h_A r_1 \Delta L}} \tag{6.8}$$

Following the algorithm, Figure 6.1, next step consists of calculating the heat load for each fluid. The heat load for each fluid is basically adding the heat values from the tube walls heat transfer. It is very important to be very careful with the signs and follow always the same sign criterion when dealing with heat transfer equations. If not, results may not be as expected. One must also take into account that fluids flow counter-current with each other which is reflected with the sign − for heat loads $Q_1$ and $Q_3$. Otherwise, it would be a co-current situation. In this case, the heat load for each fluid is calculated as it follows:

$$\begin{gathered} Q_1 = -(Q_{\mathrm{w1}} - Q_{\mathrm{w2}}) \\ Q_2 = Q_{\mathrm{w2}} - Q_{\mathrm{w3}} \\ Q_3 = -(Q_{\mathrm{w3}} - Q_{\mathrm{w4}}) \\ Q_4 = Q_{\mathrm{w4}} \end{gathered}$$

After the heat load for each fluid is known, one can calculate the temperature increase or decrease in an element using equation 6.9.

$$Q_i = G_i Cp_i \Delta T_i \tag{6.9}$$

Where the subindex $i$ is the fluid number.

With the $\Delta T$ calculated, the new bulk temperatures at the beginning of the next element for each fluid can be known as shown in equation 6.10.

$$T_{\mathrm{b},n+1} = T_{\mathrm{b},n} + \Delta T_{\mathrm{b}} \tag{6.10}$$

Where $T_{\mathrm{b},n+1}$ is the new bulk temperature for the next element and $T_{\mathrm{b},n}$ is the bulk temperature of the present element.

The average wall temperatures are also updated considering that the average wall temperature at the beginning of the new element is the same as the average wall temperature calculated in the present element. After all temperatures are updated and thus, all the calculations for the present element are finished, it is time to move forward and repeat the previous procedure for the next element. When the calculations reach *leg1*, special temperatures must be taken into account. Moreover, when the last element is reached, certain bulk temperatures must be compared, see Figure 6.1. The most important one is that the calculated bulk temperature from the utility side is close enough to the ingoing set value defined. If the difference between temperatures is higher than the defined tolerance, then new bulk temperatures must be guessed and a new iteration through the whole unit must be performed until they converge according to the tolerance set. If the temperatures have already converged, heat calculations are finished and the fluids' temperatures are plotted obtaining the temperature profile for the VLA heat exchanger.

## 6.2. Pressure Drop

Due to the VLA's geometry (annular cross-sectional area) and that the heat exchanger deals with both Newtonian (water) and non-Newtonian fluids (mainly food products), there is not a specific Fanning's friction equation that describes perfectly the friction factors and thus, the primary pressure drop in the heat exchanger. For this reason, a literature study has been done in this field. From this study, different correlations have been found although most equations are for circular ducts and Newtonian fluids ([3], [13], [10], [14] and [11]). Moreover, one must take into consideration that the VLA is for very viscous fluids which is not always considered in all expressions and turns into a difficulty when looking for information. Although non-Newtonian fluids are quite common and annular geometry as well, there is still not much material. Different expressions obtained from the literature study have been tested in order to see which describes better the primary pressure drop in the heat transfer unit. Furthermore, the singular pressure drops must be also calculated which means that the $\xi$ factors must be known.

In Figure 6.5, the pressure drop algorithm developed in the code is shown. This algorithm is simpler than the heat transfer algorithm developed for this unit as no iteration is needed. For each tube ($n$ is the tube number), the pressure drop is calculated and to do so, each tube has been divided into different intervals according to the cross-sectional area. This is done mainly because as the cross-sectional areas can be circular or annular, the hydraulic diameters are different and thus, the velocity and other values differ. As well as in the heat transfer algorithm, the unit has been discretized in the same way which means that the number of elements (total length of the pipe divided by the number of steps, defined by the user) is the same. Calculations proceed in the same manner as in the heat transfer, for every single element along the VLA's length. The first thing is to locate the absolute element's length in the corresponding length interval. Then, for each interval, the hydraulic diameter is defined and thus, the cross-sectional area ($A$) and the Reynolds number for each element can be calculated. Once the Reynolds number is known, it is evaluated so that the fluid regime can be determined and thus, use the correct correlation for calculating the friction factor. There are different friction factor correlations regarding the fluid regime which the user can select through the program's interface.

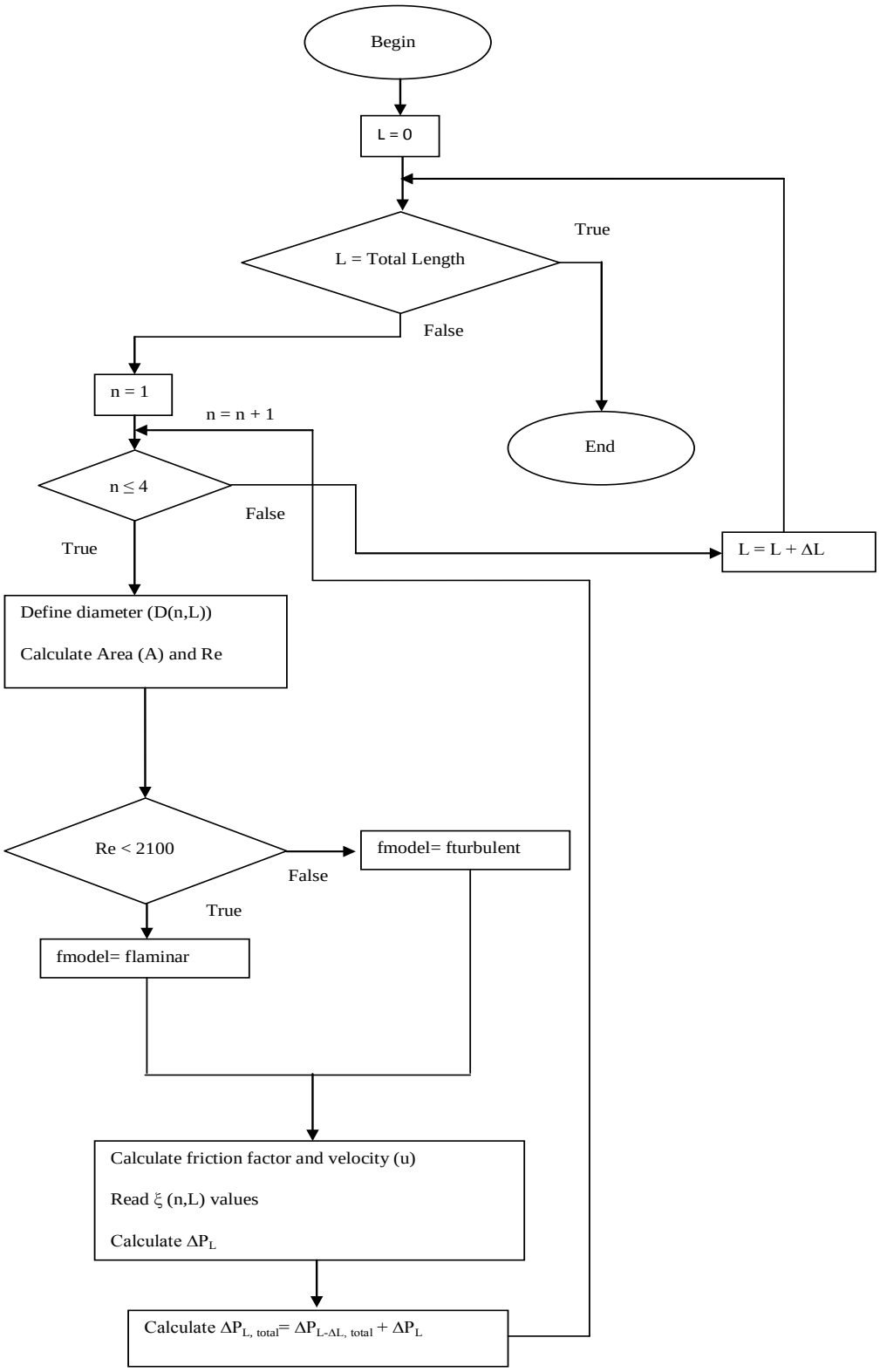


Figure 6.5: VLA's Pressure Drop Algorithm

### Laminar flow

For laminar flow, different expressions for the friction factor were found. Apart from equation 4.29, which is for circular pipes, the other expressions are the following:

- Idelchik's expression: annular duct [3]

$$\lambda_{\text{non-C}} = k_{\text{non-C}}\lambda \tag{6.11}$$

$$k_{\text{non-C}} = \frac{1 - \left(\frac{D_\text{i}}{D_\text{o}}\right)^2}{1 + \left(\frac{D_\text{i}}{D_\text{o}}\right)^2 + \frac{\left[1-\left(\frac{D_\text{i}}{D_\text{o}}\right)^2\right]}{\ln\frac{D_\text{i}}{D_\text{o}}}} \tag{6.12}$$

  Where $\lambda$ is the Darcy–Weisbach's friction factor calculated from equation 4.26 and equation 4.27. $D_\text{i}$ is the external diameter of the inner cylinder and $D_\text{o}$ is the internal diameter of the outer cylinder for two coaxial cylinders.

- Newtonian fluid expression for flat plates [13]

$$f = \frac{24}{Re} \tag{6.13}$$

- Non-Newtonian (power-law) fluid expression for flat plates [13]

$$f = \frac{24}{Re_\text{e}}\left[\frac{2n+1}{3n}\right] \tag{6.14}$$

$$Re_\text{e} = \frac{2\rho s u}{\mu_\text{e}} \tag{6.15}$$

$$\mu_\text{e} = K\left(\frac{u}{s}\right)^{n-1}\left[\frac{2+4n}{n}\right]^{n-1} \tag{6.16}$$

  Where $n$ is the power-law fluid index, $s$ is the distance between plates [m], $u$ is the local velocity [m/s] and $\rho$ is the fluid's density [kg/m$^3$].

- Churchill equation: circular pipe ([10] and [14])

$$f = 2\left[\left(\frac{8}{Re}\right)^{12} + \frac{1}{(A+B)^{\frac{3}{2}}}\right]^{\frac{1}{12}} \tag{6.17}$$

$$A = \left(-2{,}457\ln\left[\left(\frac{7}{Re}\right)^{0{,}9} + \frac{0{,}27\epsilon}{D}\right]\right)^{16} \tag{6.18}$$

$$B = \left(\frac{37530}{Re}\right)^{16} \tag{6.19}$$

  Where $D$ is the pipe's diameter and $\epsilon$ is the pipe's roughness, both in [m].

- Soursop's friction factor: concentric annuli and power-law fluid [11]

$$\xi(\kappa) = \frac{8(1-\kappa)^2}{\frac{1-\kappa^2}{\ln\kappa} + 1 + \kappa^2} \tag{6.20}$$

Where $\kappa$ is the annulus aspect ratio ($R_\mathrm{i}/R$), $R_\mathrm{i}$ is the external radius of the inner cylinder and R is the internal radius of the outer cylinder for two coaxial cylinders.

$$\upsilon = \frac{24}{\xi} \tag{6.21}$$

$$\phi(n) = \frac{\upsilon n + 1}{(\upsilon + 1)n} \tag{6.22}$$

$$Re_\mathrm{g} = \frac{\rho \overline{v}_z{}^{2-n} D_\mathrm{h}{}^n}{K[\phi(n)]^n[\xi(\kappa)]^{n-1}} \tag{6.23}$$

$$f = \frac{2\xi}{Re_\mathrm{g}} \tag{6.24}$$

The soursop's friction factor expressions were derived by Gratão et al. [11] due to the fact that in many fluid-flow and heat transfer devices, the annular space is an important geometry. Moreover, the soursop juice had been chosen as fluid test due to its rheological behavior (shear-thinning fluid) and its potential for the international market, specially in South America [11].

**Turbulent flow**

- Swamee–Jain equation [2]

$$f = \frac{0{,}25}{[\log(\frac{\epsilon}{3{,}7D} + \frac{5{,}74}{Re^{0{,}9}})]^2} \tag{6.25}$$

- Idelchik's expression: annular duct [3]

$$\lambda_\mathrm{non-c} = \left(\frac{0{,}02 D_\mathrm{i}}{D_\mathrm{o}} + 0{,}98\right)\left(\frac{1}{\lambda} - 0{,}27\frac{D_\mathrm{i}}{D_\mathrm{o}} + 0{,}1\right) \tag{6.26}$$

- Idelchik's expression: circular duct [3]

$$\lambda = \frac{1}{(1{,}8\log Re - 1{,}64)^2} \tag{6.27}$$

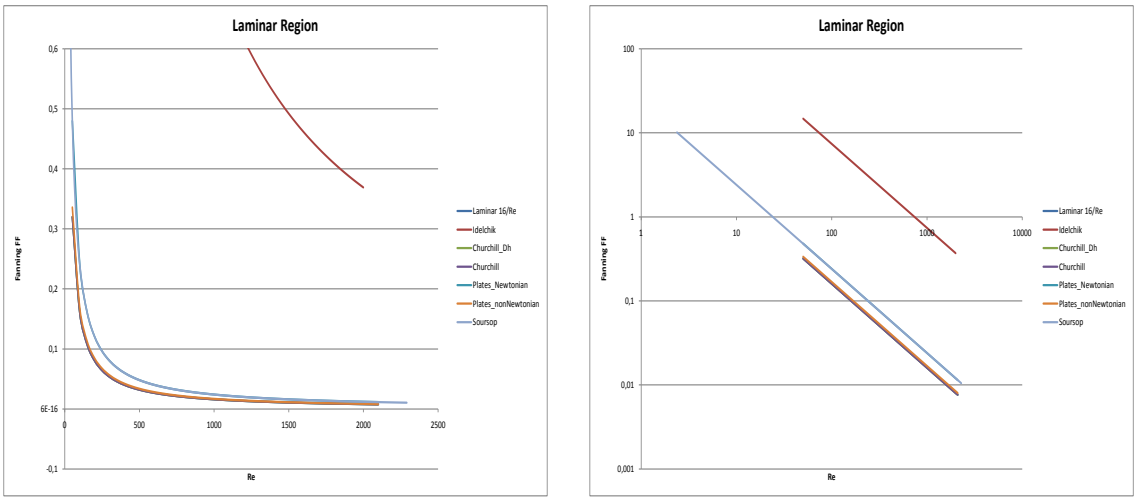


(a) Linear scale (b) Logarithmic scale

Figure 6.6: Friction factor correlations for laminar flow

First of all, these equations have been evaluated and plotted to see their tendencies. For laminar flow, the results are the following, see Figure 6.6.
As it can be seen, almost all the laminar equations used follow the same tendency and have close values except for Idelchik's equation, equation 6.12. Idelchik's equation deviates more than in a factor of 10 from the other values and for this reason, it is rejected for modeling the VLA's pressure drop. It is unknown why there is such a big difference between Idelchik's equation and the rest but a possibility can be a typographical error.

However, results for the turbulent flow do not differ that much from laminar's results. As it can be seen in Figure 6.7, there is also a large difference between Idelchik's correlation and the rest. Moreover, in Idelchik's equation, Fanning's friction factor increases with increasing Reynold's number meanwhile in the other correlations, Fanning's friction factor decreases with increasing Reynold's number. Nevertheless, between the other equations there is also some difference while in the laminar regime, values were similar. Looking into detail in the turbulent region discarding Idelchik's equation, there are some things to point out. Colebrook–White's equation for a circular pipe presents the same function independent of the pipe roughness while Colebrook–White's equation for an annular pipe presents different functions according to the pipe's roughness. As the pipe's roughness decreases, with increasing Reynold's number, Fanning's friction factor decreases faster. Swamee–Jain's equations present similar functions disregarding the pipe's roughness and present almost the same values as Colebrook–White's expression for an annular pipe with $\epsilon = 1 \cdot 10^{-6}$m. Furthermore, in the lower part of the figure there are two more functions that correspond to Churchill's correlations for circular and annular pipe and Idelchik's correlation for a circular pipe. Both Churhill's correlations show the

same tendency.

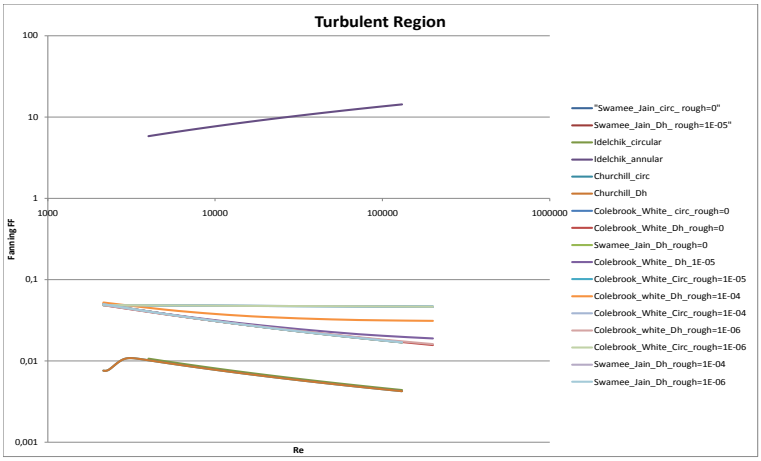


Figure 6.7: Friction factor correlations for turbulent flow

Once the friction factor has been determined, the singular pressure drop coefficients, different values according to the intervals, must be evaluated. Different methods exist for calculating these coefficients.

### Singular pressure drop coefficients or $\xi$ factors

For modeling the pressure drop in the heat exchanger unit, apart from calculating the primary pressure drops, one must take into account the pressure drop due to turns, transitions, etc. From the VLA's geometry it is obvious that the singular or secondary pressure drops must also be considered. For calculating singular pressure drops, the $\xi$ factors (singular pressure drop coefficients) for each singularity in the heat exchanger must be known. As mentioned in the theory part, the $\xi$ factors depend mainly on the geometry of the singularity and thus, there are different ways of obtaining these values. In this project the $\xi$ factors have been obtained by two procedures; one is by consulting tables and graphics and the other one is by performing a Computational Fluid Dynamics (CFD) analysis. In the following table, Table 6.1, the values from both tables and graphics and the CFD analysis are compared. For a better comprehension of the element referred, one can consult the VLA sketch, see Figure 5.1. However, the CFD analysis could not be performed through all the elements in the unit due to a lack of time.

In [18], contractions or expansions inside a pipe are calculated as it follows:

- Expansion

$$\xi = \left(1 - \beta^2\right)^2 \tag{6.28}$$

Table 6.1: $\xi$ factors

| **Element** | | **$\xi$ Calculated value** | **$\xi$ CFD value** | **Reference** |
|---|---|---|---|---|
| Tube 1- Pipe | *Contraction* | 0,25 | | [18] |
| | *Expansion* | 0,26 | | [18] |
| Tube 1 - Tube 4 | *Contraction* | 0,23 | 5,8 - 7,5 | [18] |
| | *Expansion* | 0,21 | 5,7 - 6,6 | [18] |
| Tube 1 - Tube 3 | *Pumping* | 1,8 | | [3] p.401 |
| | *Suction* | 0,4 | | [3] p.402 |
| Tube 3: circular - annular | *Contraction* | 0,29 | 2,32 - 5,43 | [18] |
| | *Expansion* | 0,33 | | [18] |
| Tube 4: 3 bends | | 1,4 | | [18] |
| Tube 2 - pipe | *Contraction* | 0,13 | | [3] p.317 |
| | *Expansion* | 0,45 | | [3]p.278 |
| Tube 2: circular - annular | *Contraction* | 0,023 | | [18] |
| | *Expansion* | 0,21 | | [18] |
| Tube 2: 180° bend | | 1 | 2,04 - 7,13 | [18] |
| 90° bend | | 0,3 | | [18] |

- Contraction

$$\xi = 0{,}5\left(1-\beta^2\right) \tag{6.29}$$

Where $\beta$ is the ratio between the small diameter and the big one.

When comparing the $\xi$ factors from the bibliography with the ones obtained from the CFD analysis, a notable difference is observed. It is not known why the difference between methods is so large but when calculating the pressure drop with the CFD values, the pressure drops are higher than the values obtained when using the $\xi$ factors from literature and differ a lot. However, these results were totally unexpected as the CFD analysis should be more accurate as one can obtain a correlation for a determined geometry rather than a constant value obtained from literature. Due to this unexpected result, the lack of time and that the pressure drops calculated with the constant values fitted very well to the real data, no more CFD analysis were performed.

After having calculated the friction factor and the $\xi$ factors, the pressure drop for the corresponding element must be calculated using both equation 4.26 and 4.33 which results in the following equation.

$$\Delta P_{(1-2)[k,\text{element}]} = \Delta P_{(1-2)\text{p}} + \Delta P_{(1-2)\text{s}} = \left(4f\frac{\Delta L}{D} + \xi\right)\rho\frac{u^2}{2} \tag{6.30}$$

Where $\Delta L$ is the element's length, $k$ is the element number and $u$ is the fluid's velocity at the smallest cross-sectional area.

Once the total pressure drop for the element is calculated, the accumulated or total pressure drop of the VLA till the absolute element's length can be known by adding the element's calculated pressure drop to the accumulated one through the unit.

$$\Delta P_{(1-2)[k,\text{total}]} = \Delta P_{(1-2)[k-1,\text{total}]} + \Delta P_{(1-2)[k,\text{element}]} \tag{6.31}$$

This procedure must be repeated through the whole unit length to obtain the total pressure drop for each tube and for the product and the utility side.

# 7. Results

In this chapter, the elaborated code is evaluated with the experimental data from the tests done in the laboratory in order to determine if the code is reliable enough to be further used by Alfa Laval for commercial purposes. In order to compare all the available results, this chapter is divided into a heat transfer section and a pressure drop section as they are two things modeled independently. Moreover, there is a third section dedicated to the non-Newtonian fluids.

To be able to evaluate the generated code, the experimental data obtained from the laboratory tests have been compared to the code results, using the test data as input data. This means that the input data in the heat exchanger are the same for the laboratory tests and the code evaluation and the output data are the values needed for the comparison.

Different tests were run, see Table 5.1. Nevertheless, not all the data has been evaluated. Insert 11 is the only insert that has been completely evaluated; pressure drop and heat transfer for both water and oil tests. Insert 11 with mixers was withdrawn from the test for technical reasons. Nonetheless, for item 14, the data for the water test was evaluated. Although the heat transfer data showed good results, pressure drops needed some adjustments and due to the lack of time, it was preferred to perform a complete analysis on insert 11.

## 7.1. Heat Transfer

To evaluate the validity of the code's heat transfer calculations for the VLA, two different tests were run. The first one was using water on both sides of the unit (water as product and as utility, water/water) and the second one was using oil as product and water as the utility fluid (oil/water). In both cases, the code evaluation procedure followed was the same. It was chosen to set as variables to compare the outgoing temperatures of the VLA and the heat loads for each fluid as they allow to obtain a general idea of what happens in the heat exchanger. First, the data was obtained from the laboratory. These data contained the ingoing and outgoing temperatures as well as the flow rates of both fluids and the pressure drop for both sides. As heat transfer is evaluated, pressure drop data will not be matter of interest in this section. Once the data are obtained, the average temperature between the ingoing and the outgoing temperature for each fluid, the product and the utility, is

calculated. With the average temperatures obtained, the specific heat at constant pressure ($C_p$) for each fluid is calculated and thus, the heat load for each side is calculated using equation $Q = GC_p\Delta T$, equation 6.9.

After dealing with the test data, it is time to run the code. Using as input data to the code the input test data, the outgoing temperatures are calculated. As mentioned in Chapter 6, different Nusselt correlations can be chosen to calculate the heat transfer in the VLA. Different correlations exist depending on the flow regime and the type of fluid, Newtonian or non-Newtonian. Once the outgoing temperatures from the code are calculated, the same evaluation procedure (average temperature, $C_p$ and heat loads for each fluid) is done.

When the data evaluation procedure is finished, the results obtained, outgoing temperatures and heat loads, can be compared.

### 7.1.1. Water/Water

The water/water case, water both on the product and on the utility side, was the first case tested in the laboratory and due to the fluid's properties, Newtonian and turbulent flow, it should be the one presenting less problems when modeling. In the following figures, the chosen variables defined previously are compared. The test consisted in cooling water (product) from 50°C with water (utility) at 30°C covering a $Re$ range for the product side between $[5200 - 90000]$. The aim of this test is to simulate a CIP (Cleaning In Place) operation where water at high flow rates is used for cleaning the product side. For item 14 and item 11 with mixers, the same ingoing temperatures were used but the Reynolds product range was between $[21500 - 184000]$ and $[5000 - 66000]$ respectively.

In the first graph, Figure 7.1, the outgoing product temperature, which is water, calculated with the code ($T\_CODE$) is plotted versus the outgoing temperatures obtained from the laboratory test ($T\_TEST$) for the two available correlations. As water is run in both sides under turbulent flow, the two available correlations will be tested to see which one gives a better estimation when comparing to the experimental data. These correlations are Monrad and Pelton (MP, equation 6.6) and Dittus–Boelter (DB, equation 4.14). If the calculated temperatures were the same as the ones from the laboratory, all the points should be plotted in the diagonal. However, it is not the case although the temperatures calculated using Monrad and Pelton's correlation are almost on the diagonal. Dittus–Boelter's points present a higher deviation from the ideal situation than Monrad and Pelton's. Monrad–Pelton's deviation is less than 0,2 K and Dittus–Boelter's deviation is less than 1,1 K which leads to the conclusion that both correlations give accurate results and that the elaborated code is reliable.

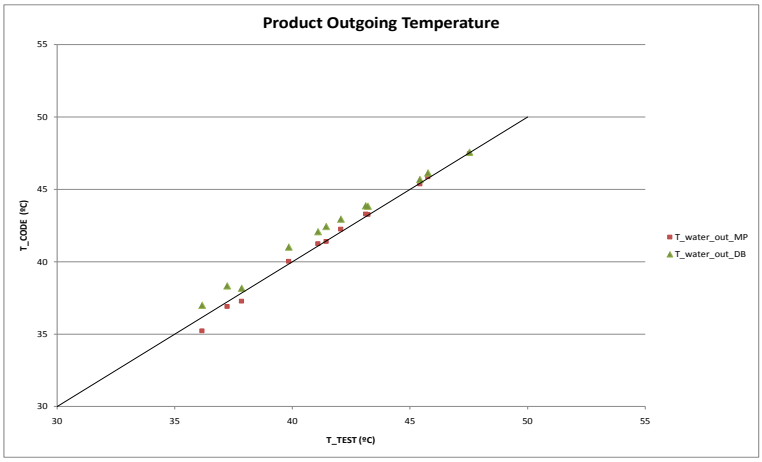


Figure 7.1: Outgoing product temperature for the water/water test

For the utility side, the results for the outgoing temperature are very similar to the ones obtained for the product side. As seen in Figure 7.2, the values calculated using Monrad and Pelton's correlation are closer to the ideal situation in which the values obtained from the code are the same as the ones obtained from the tests than with Dittus–Boelter's equation. Nevertheless, the difference between the two correlations and the ideal situation is not significant (1,2 K the highest) and thus, both correlations are valid.

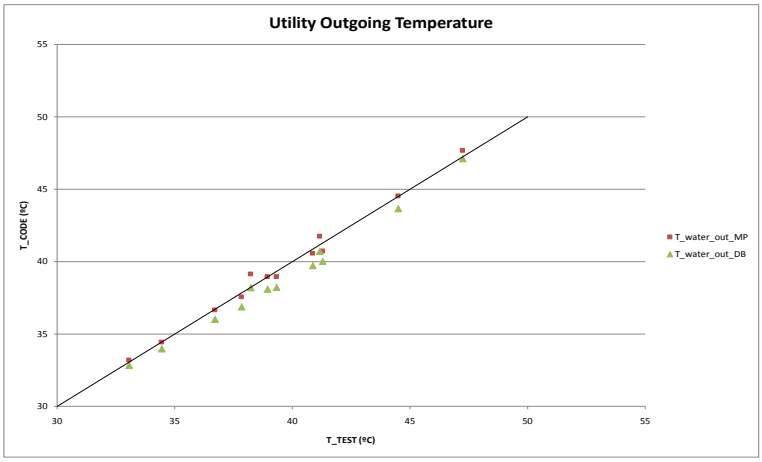


Figure 7.2: Outgoing utility temperature for the water/water test

Before proceeding with comparing heat loads, first, the tested data must be evaluated. In this case, see Figure 7.3, the product heat load ($Q$) has been plotted versus the utility heat load. As it can be seen, values are placed in the graph's diagonal

which means that the heat load for both sides are the same and thus, it seems reasonable to calculate an average heat load to continue with the calculations. As the heat load for the utility and the product side are the same, both should have the same weight in the expression and thus, the average heat load $\langle Q \rangle$ used is calculated as it follows:

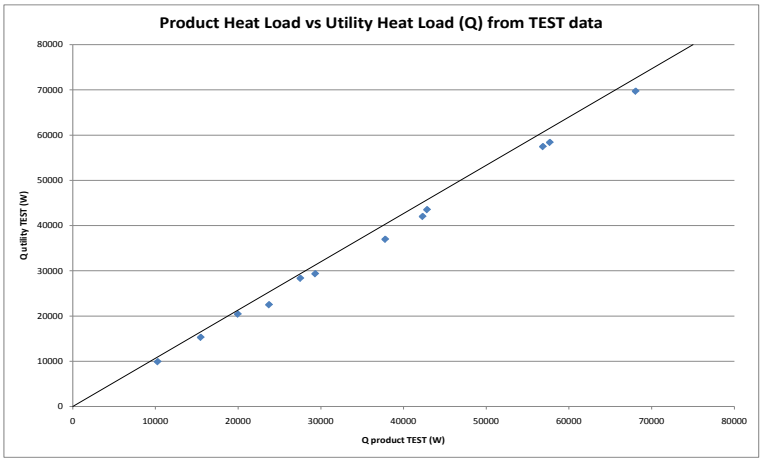


Figure 7.3: Heat load comparison for test data for the water/water test

$$\langle Q \rangle = \frac{Q_{\mathrm{p}} \left|\Delta T_{\mathrm{p}}\right| + Q_{\mathrm{u}} \left|\Delta T_{\mathrm{u}}\right|}{\left|\Delta T_{\mathrm{p}}\right| + \left|\Delta T_{\mathrm{u}}\right|} \tag{7.1}$$

Where:

$Q_{\mathrm{p}}$ and $Q_{\mathrm{u}}$ are the product and the utility heat loads, [W]

$|\Delta T_{\mathrm{p}}|$ and $|\Delta T_{\mathrm{u}}|$ are the absolute temperature difference between the way in and the way out for the product and the utility side, respectively

In the following graph, Figure 7.4, the average heat load $\langle Q \rangle$ obtained from the calculated code data ($\langle Q \rangle \, CODE$) is plotted versus the average heat load calculated from the test data ($\langle Q \rangle \, TEST$). Due to the fact that the fluid is water run under turbulent flow for both sides and that only two correlations are available to calculate the average heat load within the code, it means there are four possible combinations (product/utility): Monrad–Pelton/ Monrad–Pelton, Monrad–Pelton/ Dittus–Boelter, Dittus–Boelter/ Monrad–Pelton and Dittus–Boelter/ Dittus–Boelter. However, due to the good results obtained from just considering the same correlations for both sides and the fact that this model should be for non-Newtonian fluids and not water, the other two cases were not taken into consideration. Looking into detail into Figure 7.4, no significant difference can be observed between the two correlations although it seems that Monrad and Pelton's correlation provides closer results to real life situation but more experiments should be done for differentiating the two correlations.

The previous results show that when using water as product and utility both under turbulent conditions, the elaborated code provides very good heat transfer estimations of what happens in the VLA. Also, the two available Nusselt correlations (Monrad–Pelton and Dittus–Boelter) proved to be suitable for modeling the heat transfer. One must take into account that Monrad and Pelton's correlation is for annular ducts but Dittus–Boelter's one was designed for circular ducts and has been adapted to an annular geometry by substituting the circular diameter for the hydraulic diameter. One could expect worse results as the correlation has been adapted and not used in its proper context but it turned up that it also worked for this geometry.

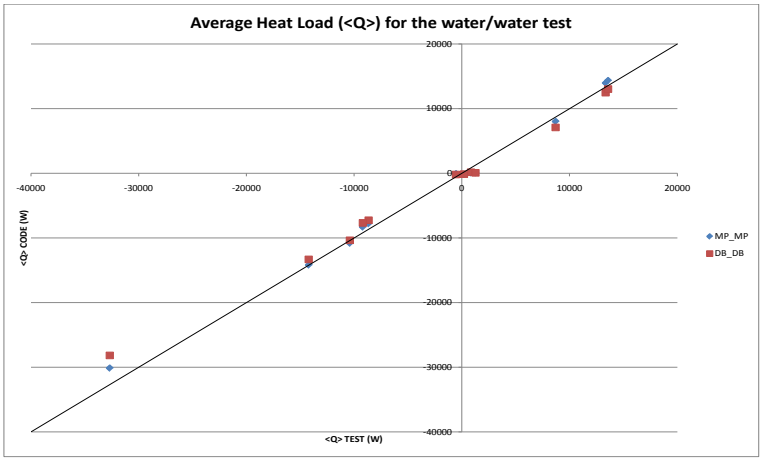


Figure 7.4: Average Heat load for the water/water test

To sum up, the heat transfer model designed is suitable for the VLA heat exchanger when using water as product in turbulent flow.

### 7.1.2. Oil/Water

The other test performed in the ViscoLine Annular heat exchanger was using oil as product and water as utility. Although oil is a Newtonian fluid, it is more viscous than water and thus, it is an intermediate case between water and a power-law fluid. Two different runs were done in the unit, first, oil around 37°C was cooled down using water at around 15°C and afterwards, oil at around 14°C was heated with water at around 35°C. For both heating and cooling, oil was under laminar regime covering the following Reynolds ranges: $Re_{\text{cooling}} : [5{,}5 - 136]$ and $Re_{\text{heating}} : [5 - 80]$. In the utility side, water remained under turbulent flow. For item 14, the same Reynolds numbers and temperatures were used.

Using oil under laminar regime and according to the available Nusselt correlations in the code for laminar flow, see Chapter 6, there are three possible correlations: Sieder and Tate (ST, equation 6.1), Hausen (H, equation 6.2) and Stephan (S, equation 6.3). For the utility side, as water is turbulent, the same correlations as in the water/water test are used; Monrad and Pelton (MP) and Dittus–Boelter (DB). An increasing number of available correlations leads to an increasing number of possibilities: ST/MP, ST/DB, H/MP, etc. up to the number of six.

Due to the number of possibilities and that the outgoing temperatures are related to heat loads, outgoing temperatures will only be plotted in some cases. For this reason, heat loads will be treated first.

Following the same procedure as done with the water/water test, the product test heat load is plotted against the utility test heat load, see Figure 7.5. Comparing this graph with Figure 7.3, the same graph for the water/water test, it can be seen that most values deviate more from the equal heat load situation. Moreover, when looking into detail into the results, this fact is verified. For this reason, it would be treacherous to calculate an arithmetic average heat load. There are different ways of comparing the measured heat loads with the calculated ones. In this case, it is chosen to represent the calculated utility heat load versus the heat load obtained from the tests data for the different product Nusselt correlation cases. This means that for each product correlation (there are three), the utility heat load calculated using Monrad–Pelton and the utility heat load calculated by Dittus–Boelter are plotted. It was chosen to represent the utility heat load from the water/water test because it is verified that heat transfer under turbulent conditions for water works while there is no previous information about the calculations for oil under laminar flow although $\Delta T_{H_2O}$ is smaller now. Besides, all calculations are performed with Churchill's correlation for the friction factor calculations as it was the one which showed better results in the water/water test, see Section 7.2. This choice is not supposed to affect the results as pressure drop is independent of heat transfer apart from a change in the physical properties.

The first figure from the oil/water test, see Figure 7.6, corresponds to the measured utility heat load versus the utility heat load obtained from the tests data when using Sieder–Tate's Nusselt correlation in the product side. As it can be seen, both possible combinations; ST/MP or ST/DB show almost the same results for cooling or heating the oil which makes it difficult to discern between which combination provides best results. Yet, both combinations present very good results as data is nearly on the diagonal and almost all values are below the 10% deviation line.

The second figure, Figure 7.7, the heat loads obtained from the calculated data and from the tests data are compared when using Hausen's correlation in the product side. In this case, despite the fact that there is no difference between the two present combinations as before; H/MP or H/DB, the calculated values heat loads using these

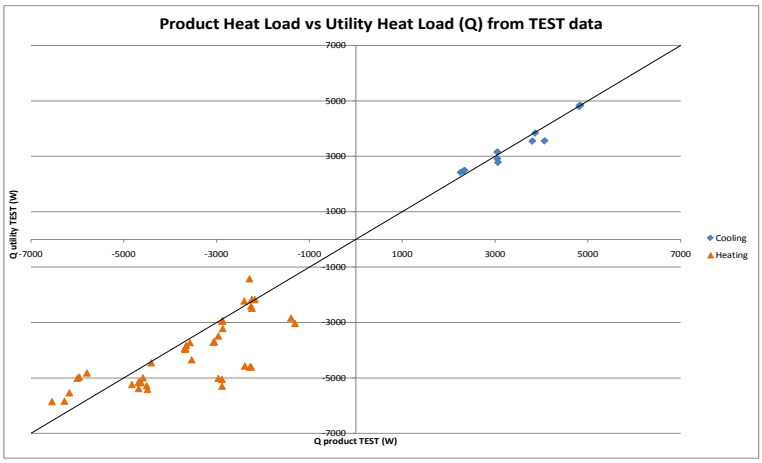


Figure 7.5: Heat load comparison for test data for the oil/water test

combinations are lower than those obtained from the test data. Most heating values lay above the –15% deviation.

The third figure, Figure 7.8, shows the comparison between the utility heat load obtained from calculated data and the utility heat load obtained from experimental data using Stephan's correlation in the product side. Again, no difference is observed between the combination Stephan/Monrad–Pelton or Stephan/Dittus–Boelter but the calculated utility heat loads when using Stephan's correlation are lower than those obtained when using Sieder Tate or Hausen, –40% deviation from the diagonal.

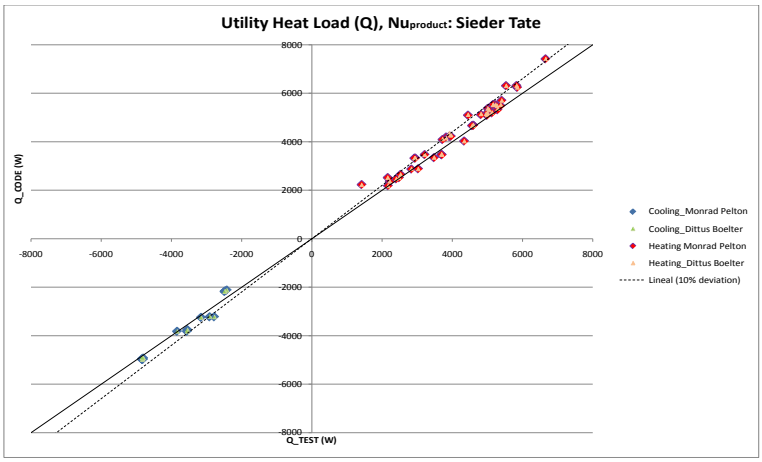


Figure 7.6: Utility heat load with Sieder Tate's correlation on the product side, oil/water test

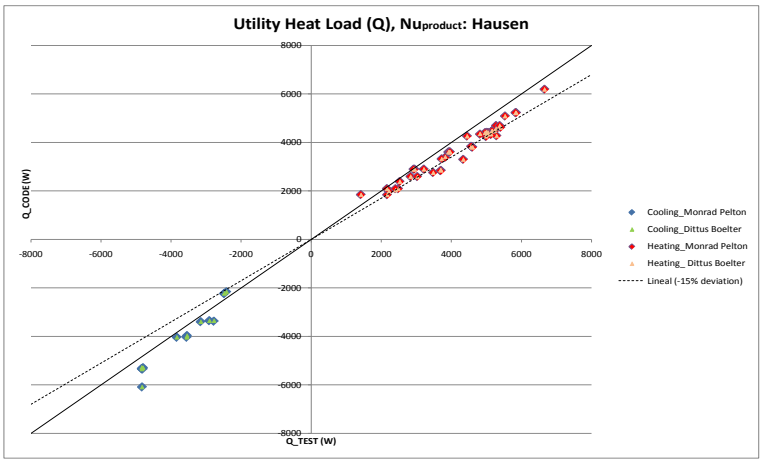


Figure 7.7: Utility heat load with Hausen's correlation on the product side, oil/water test

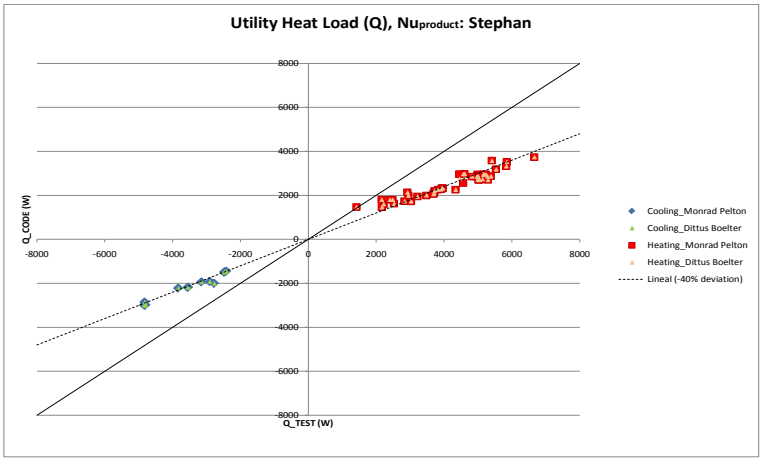


Figure 7.8: Utility heat load with Stephan's correlation on the product side, oil/water test

To sum up, the combination that provides better heat transfer estimations in the VLA is using Sieder–Tate in the product side for laminar flow either with Monrad–Pelton or with Dittus–Boelter in the turbulent utility side as no evident difference was observed between them. The other combinations estimate lower heat loads than those expected from the tested data.

Nevertheless, the Nusselt correlations for laminar flow; Sieder–Tate, Hausen and Stephan, are the average Nusselt number expressions considering the thermal entrance effect. As heat transfer is calculated in every single element in which the VLA is being discretized, local $Nu$ numbers are of interest. To calculate the local Nusselt number:

$$\overline{Nu} = \frac{1}{L}\int_0^L Nu_x dx \tag{7.2}$$

Where $\overline{Nu}$ is the length-averaged Nusselt number and $Nu_x$ is the local Nusselt number.

An average $Nu$ correlation for laminar flow has the form:

$$\overline{Nu} = AL^{-\frac{1}{3}} \tag{7.3}$$

By matching equation 7.4 with equation 7.3 and by rearranging some terms:

$$\int_0^L Nu_x dx = AL^{\frac{2}{3}} \tag{7.4}$$

Differentiating both sides of the equality:

$$Nu_x = \frac{2}{3}AL^{-\frac{1}{3}} = \frac{2}{3}\overline{Nu} \tag{7.5}$$

Thus, the local Nusselt number is $\frac{2}{3}$ of the average Nusselt number. For turbulent flow, this is not true as the average $Nu$ correlations are not dependent on the length ($L$) due to the fact that the flow and the thermal boundary layer are completely developed close to the entrance, so no entrance length effect is considered and for this reason, the average and the local Nusselt numbers share the same expression.

Taking into account the relationship between the local and the average Nusselt number, heat load calculations were performed and plotted again resulting in Figure 7.9, Figure 7.10 and Figure 7.11. If now the heat transfer is calculated using $\frac{2}{3}$ of the average Nusselt number, it means that the heat transfer coefficient will be $\frac{1}{3}$ smaller and the heat load as well since the product side is rate limiting. Certainly, this is reflected in all the graphs. All possible combinations show that the calculated utility heat load is lower than the one obtained from the test data as it was expected. Moreover, as a constant factor was introduced, no other variations are observed; values follow the same tendencies and there is no significant difference between the utility Nusselt correlations for a specific laminar Nusselt correlation and between the cooling and the heating cases. Even though results without the $\frac{2}{3}$ factor present better heat transfer estimations, it is not correct and thus, the following calculations done for the oil/water test are done taking into account the $\frac{2}{3}$ factor or in other words, using the local Nusselt number.

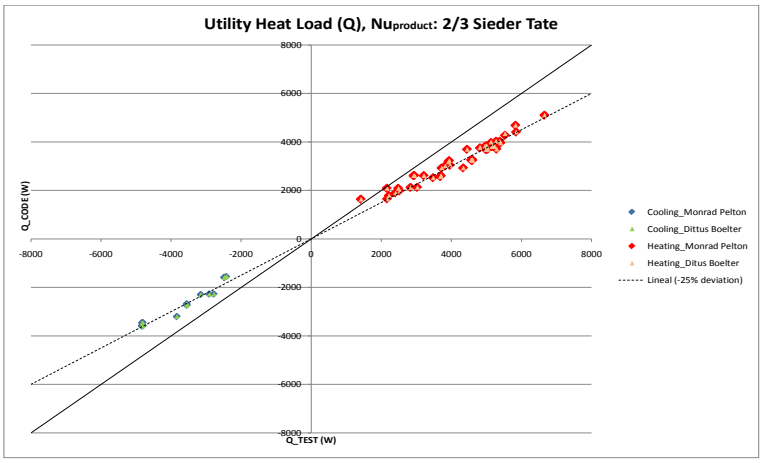


Figure 7.9: Utility heat load with Sieder Tate's local Nusselt correlation on the product side, oil/water test

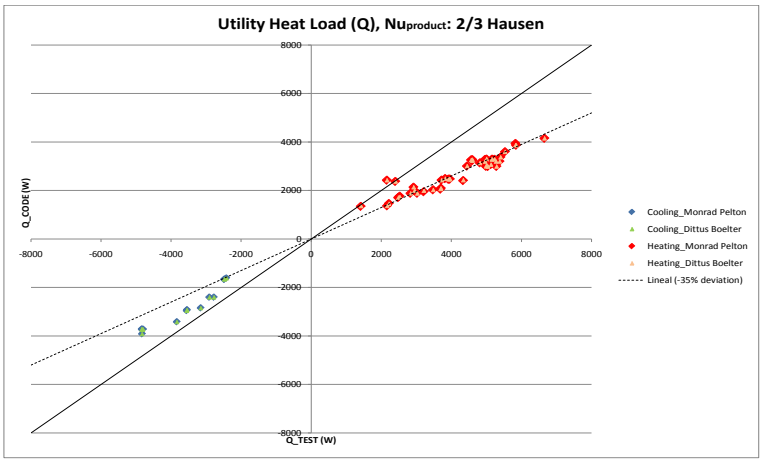


Figure 7.10: Utility heat load with Hausen's local Nusselt correlation on the product side, oil/water test

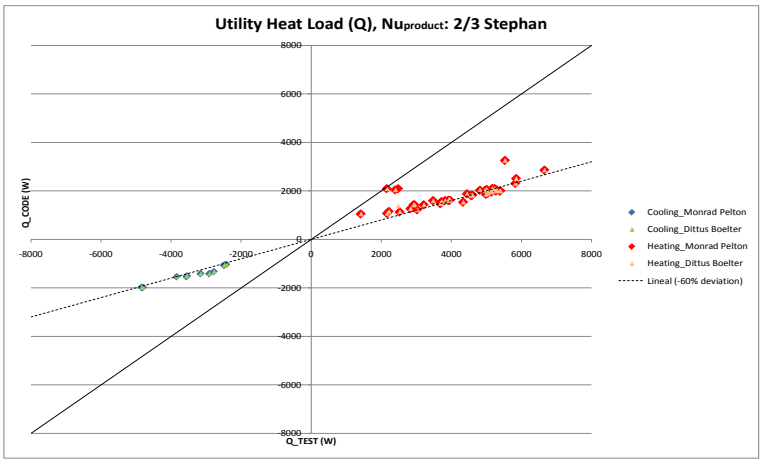


Figure 7.11: Utility heat load with Stephan's local Nusselt correlation on the product side, oil/water test

The results obtained reflect that the combination Sieder–Tate/Monrad–Pelton or Sieder–Tate/Dittus–Boelter provide the best heat transfer estimations. For this reason, the outgoing product and utility temperatures from the code and from the tests will be compared. The temperatures obtained from the code calculations are done taking into account the $\frac{2}{3}$ factor for the product side as mentioned before.

As in the previous graphs, there are no significant differences between the two possible correlation combinations and between if it is the cooling or the heating case. The calculated outgoing product temperatures plotted in Figure 7.12 present a slight deviation from the tested values while the calculated outgoing utility temperatures from Figure 7.13 can be considered as equal. Furthermore, for the product temperatures, when cooling temperatures are a bit over predicted while when heating, they are a bit under predicted. This phenomenon can also be observed with the utility temperatures but in lesser extent. However, results show that both combinations, Sieder–Tate/Monrad–Pelton and Sieder–Tate/Dittus–Boelter, provide reliable heat transfer results regardless the existing small deviations in some cases.

Anyhow, the above correlations are for a completely developed laminar flow profile considering the entrance length effect but in the VLA, it is very difficult to have an undisturbed laminar flow through the whole unit due to mainly the U-turn bend and when switching from annular to circular or vice versa. Moreover, these correlations are designed for a smooth circular pipe which in this case, it is just partially true as the tubes are smooth but there are elements like the weldings and studs that break the rule. It has been considered to calculate the heat transfer considering that a complete mixing is produced at the U-turn bend. This means considering the entrance length effect at the U-turn bend position as well as in the VLA's entrance. As Sieder–Tate's correlation was the one that provided closest results to the real life data, the different studied cases: using the global Nusselt number, using the

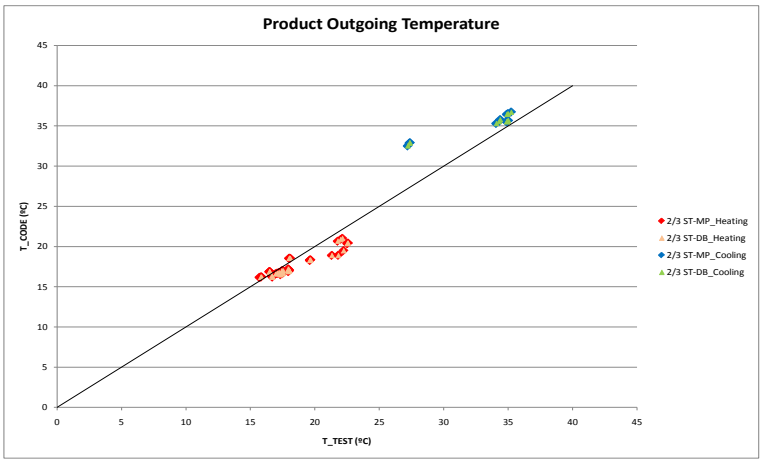


Figure 7.12: Outgoing product temperature for the oil/water test

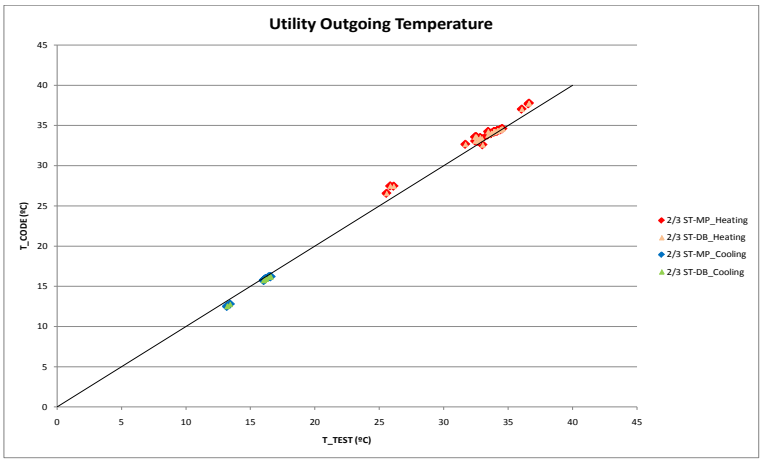


Figure 7.13: Outgoing utility temperature for the oil/water test

local Nusselt number ($\frac{2}{3}$ of the global Nusselt number) and complete mixing at the U-turn bend with the $\frac{2}{3}$ factor, have been evaluated. In the next figure, Figure 7.14, the utility heat load calculated combining the three different forms of Sieder–Tate's correlation with Monrad–Pelton have been plotted against the utility heat load obtained from the test data for the cooling and the heating cases. $ST$ refers to Sieder Tate's correlation as it is written, the average Nusselt number. $\frac{2}{3}$ $ST$ refers to the local Nusselt number and $mix$ $\frac{2}{3}$ $ST$ is when considering complete mixing at the product bend using the local Nusselt number. It was chosen to use Monrad–Pelton in the utility side as it provided good results for water under turbulent flow and it is designed for annular ducts although Dittus–Boelter could also have been suitable.

From the numbers obtained and as seen in the previous results, when using the average Nusselt number, the calculated values are almost the same as the measured

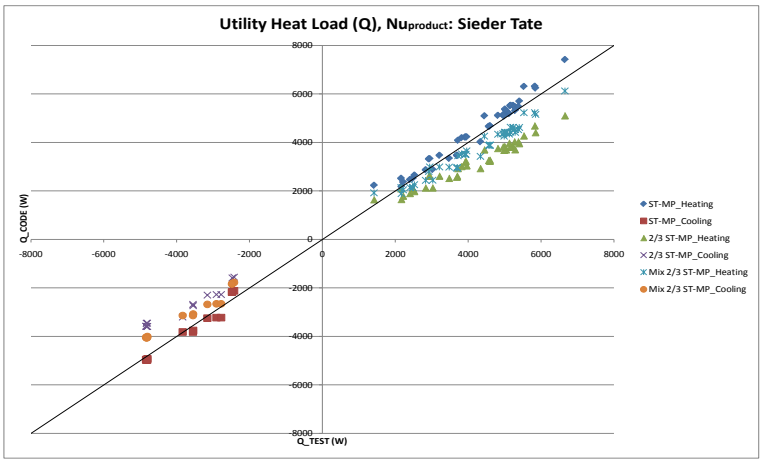


Figure 7.14: Heat load comparison for different Sieder–Tate's expressions for the oil/water test

ones. The other case is when using the local Nusselt number while when taking into account the complete mixing at half unit length, the values lay between the two other cases which is logical. However, this is just a theoretical situation as there are more points where complete mixing takes place and thus, it could be possible to obtain better results when considering them although they are difficult effects to handle.

## 7.2. Pressure Drop

To evaluate the validity of the pressure drop values obtained from the code calculations with the values obtained from the tests, a similar procedure as the one described in the heat transfer section is followed. In this case, the variables which are matter of interest for evaluating the code are the total product pressure drop and the total utility pressure drop. By total pressure drop is meant the pressure drop from the entrance till the way out of the heat exchanger.

As the data obtained from the tests and the data obtained from the code calculations all refer to the total pressure drop, no mathematical treatment of the values should be required but one must take into account the following considerations: the calculated pressure drops are just the sum of the singular and the primary pressure drops ($\Delta P_\mathrm{p} + \Delta P_\mathrm{s}$) and the pressure drop that is measured in the laboratory is the static pressure drop, $P_1 - P_2$ when looking at Bernoulli's equation, equation 4.23. This leads to the necessity of correcting one of the values in order to be able to compare them. In this project, the measured test values are the ones corrected by applying Bernoulli's equation, see equation 7.6. Now, $(\Delta P_\mathrm{p} + \Delta P_\mathrm{s})_\mathrm{c}$ can be com-

pared to $(\Delta P_{\mathrm{p}} + \Delta P_{\mathrm{s}})_{\mathrm{m}}$ meaning the subindex c calculated and m measured.

$$(\Delta P_{\mathrm{p}} + \Delta P_{\mathrm{s}})_{\mathrm{m}} = P_1 - P_2 - \frac{\rho}{2}\left(u_2^2 - u_1^2\right) \tag{7.6}$$

As well as in the heat transfer section, two test cases were run. The water/water case and the oil/water case. Besides, as also mentioned in Chapter 6, different correlations for the friction factor can be used when calculating the pressure drop according to the fluid type and the flow regime and hence, they will be evaluated to see which one presents better accuracy to the tests data. According to Bernoulli's equation 4.23, there is a factor K which is 1 for turbulent flow and 2 for laminar flow. Data were evaluated taking this factor into account but as no significant difference was observed, all calculations were performed with K=1.

### 7.2.1. Water/Water

The water/water case is the same case as described in the heat transfer results section. This means that for both product and utility side, the flow rates are turbulent and thus, the available correlations for calculating the friction factor for this flow regime and Newtonian fluids are Churchill (equation 6.17), Colebrook–White (equation 4.30) and Swamee–Jain (equation 6.25).

Although heat transfer does not matter when calculating pressure drops except for the physical properties, all pressure drop calculations were done with Monrad–Pelton's correlation as it proved to provide reliable results.

In the following figures, the calculated pressure drop $(\Delta P_{\mathrm{p}} + \Delta P_{\mathrm{s}})_{\mathrm{c}}$ or $DP\_CODE$ is plotted against the measured pressure drop $(\Delta P_{\mathrm{p}} + \Delta P_{\mathrm{s}})_{\mathrm{m}}$ or $DP\_TEST$ for the different friction factor correlations.

In Figure 7.15, the product pressure drops are plotted. As it can be seen, no substantial difference between the values from the three correlations can be observed and in addition, all values are placed in the diagonal which means that the calculated values are the same, or practically the same, as the ones measured. Anyhow, there is a point around (60000, 60000) Pa where the Colebrook–White correlation deviates from the diagonal a 9,7%. Apart from this value, the results obtained show that the three correlations and the $\xi$ constant factors used describe with success the total pressure drop for the product side.

For the utility side, the pressure drops are plotted in Figure 7.16. In this case, with increasing pressure drop test values, the calculated ones tend to deviate from the equality. Colebrook–White's correlation tends to overestimate the pressure drops

values while Churchill and Swamee–Jain correlations give basically the same results underestimating the calculated pressure drops. Despite the deviation from the ideal situation, values do not differ that much and the correlations and the $\xi$ constant factors used describe quite well the pressure drop for the utility side.

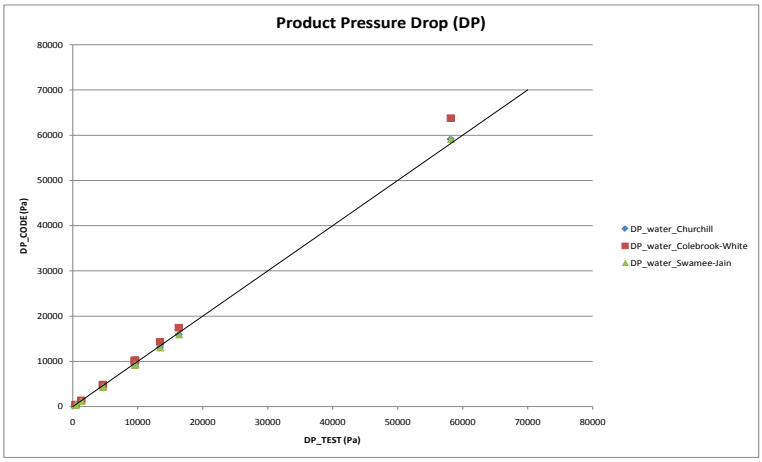


Figure 7.15: Product pressure drop for the water/water test

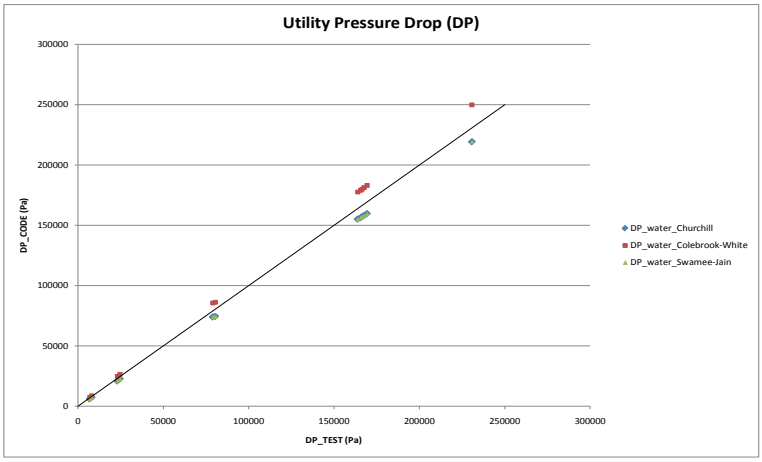


Figure 7.16: Utility pressure drop for the water/water test

### 7.2.2. Oil/Water

The oil/water test for pressure drop measures was done at the same time as for the heat transfer data. As well as with the water/water test, the calculated product and utility pressure drops will be plotted against the measured values from the test. As oil is run at low Reynolds numbers, laminar flow, the available friction factor correlations for modeling the total pressure drop are: Churchill (equation 6.17), the laminar friction expression for circular ducts, $f = 16/Re$ (equation 4.29) and the flat plates' expression for Newtonian fluids (equation 6.13). Two tests were run for the oil/water test; one cooling case and one heating case, both data will be taken into account. Besides, all pressure drop calculations were done with the local Nusselt number using Sieder–Tate's for the product side and Monrad–Pelton's correlation for the utility side although it should not affect the pressure drop results.

But not only oil is used in the VLA unit. Water is used as utility medium for cooling or heating depending on the case under turbulent flow. Thus, different friction factor correlations than the ones used for oil should be used. The friction factor correlations for turbulent flow are the same as the ones used in the water/water case: Churchill, Colebrook–White and Swamee–Jain.

In the first figure, Figure 7.17, the calculated product pressure drop ($DP\_CODE$) is plotted versus the measured product pressure drop ($DP\_TEST$). As it can be seen in the graph, Churchill and $f = 16/Re$ present the same results for the cooling and the heating case and quite close to the equality situation. However, for the cooling case, as the pressure drop increases, the calculated values deviate more from the diagonal underestimating the total pressure drop values. The other correlation, the flat plates correlation, $f = 24/Re$, presents better results for the cooling than for the heating case. It is not a bad idea to use flat plates correlations for annular ducts as it is the limiting case together with the circular cross-sectional area. Likewise, the pressure drop calculations do not depend only on the friction factor as the singular pressure drop coefficients are also present ($\xi$ factors). Thus, it means that the combination of the calculated $\xi$ factors and Churchill's and $f = 16/Re$ friction factor correlations give reliable pressure drop numbers for modeling the product pressure drop. Nevertheless, the flat plates correlation deviates more than the others because the friction factor is 1,5 times bigger and thus, this is reflected in the pressure drops. Yet, the difference observed between the heating and the cooling cases could be explained by the wall viscosity effect as it is not taken into account in the pressure drop calculations mainly because there is not much information in literature. Thanks to having access to Heat Transfer Research, Inc. publications, friction factor correction factors for the cooling and the heating cases were calculated.

- For a cooling case with a product volumetric flow rate of 0,66l $l$/s and a utility flow rate of 0,73 $l$/s, with a measured product pressure drop of 50900 Pa, a correction factor of 1,32 was obtained with equation 4.29 and thus, the

calculated pressure drop should be 36500 Pa, higher than the one obtained before (27600 Pa) but still below the expected value.

- For a heating case with a product volumetric flow rate of 1,70 $l/s$ and a utility flow rate of 1,64 $l/s$, with a measured product pressure drop of 226000 Pa, a correction factor of 0,79 was obtained with equation 4.29 and thus, the calculated pressure drop should be 185000 Pa, lower than the one obtained before (234000 Pa). In this case, the corrected value deviates more from the measured value than if no correction factor is used.

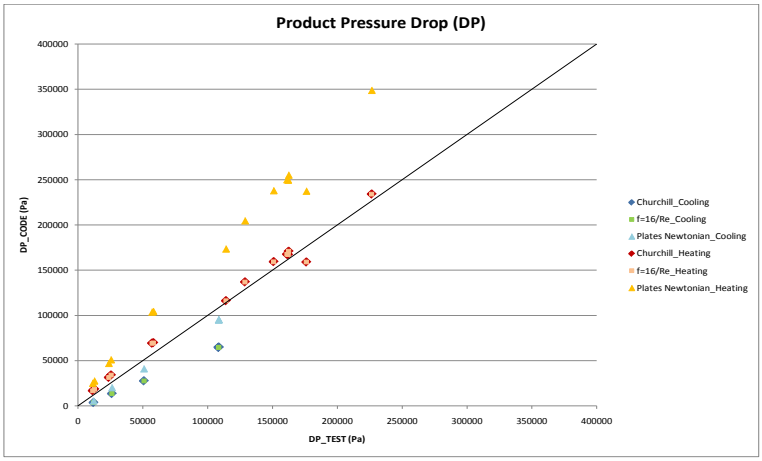


Figure 7.17: Product pressure drop for the oil/water test

The next figure, Figure 7.18, corresponds to the comparison between the calculated utility pressure drop and measured utility pressure drop. Churchill's and Swamee–Jain's correlations show the same results and the calculated pressure drop is a bit underestimated when comparing to the measured value. On the other hand, Colebrook–White's expression overestimates the calculated pressure drop. Nevertheless, the deviations from the ideal situation where the measured value is the same as the calculated one, are small enough (within the 10%) to consider the model as reliable although deviation from equality increases with increasing pressure drops. Besides, the selected correlations and the defined $\xi$ factors for the unit show that the pressure drop model defined is reliable enough for modeling the pressure drop in the Viscoline Annular heat exchanger. No evident difference between cooling and heating is observed.

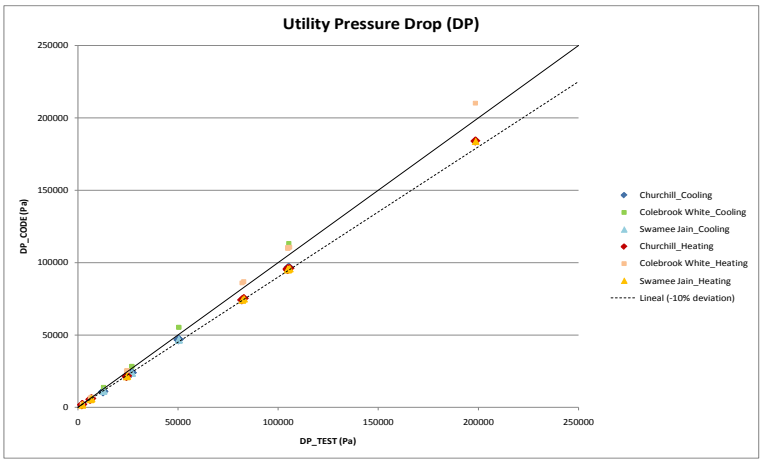


Figure 7.18: Utility pressure drop for the oil/water test

## 7.3. Non-Newtonian Fluids

The main aim of this project is to obtain a correlation that describes the heat transfer and the pressure drop for non-Newtonian fluids, especially for power-law fluids as it is mainly designed for food purees. To do so, some modifications in the elaborated code must be done to take into account the properties of this kind of fluids. Once these modifications have been done, for a range of Reynolds numbers, the code will be evaluated and afterwards, the data will be fitted into a correlation.

To be able to simulate the behavior of the non-Newtonian fluids, first, physical properties must be introduced into the code. As these properties depend on the type of fluid one is handling, there is no general expression for the density, the specific heat at constant pressure or the thermal conductivity. In this project, the physical properties used were soursop's juice properties obtained from Gratão et al. [11]. It was chosen to work with the correlations from Gratão et al. because this group had investigated about friction and heat transfer of this power-law food product in annular ducts. For this reason and also because of the lack of experiments and data regarding this field, it was decided to work with the soursop juice. The expressions are the following ([11] and [12]).

$$\rho = 981{,}4 + 4{,}54x_{\text{ss}} - 0{,}23T \tag{7.7}$$

Where:

$x_{\text{ss}}$ is the content of soluble solids, [°Brix]
$T$ is the fluid's temperature, °C
$\rho$ is the soursop's density, $\left[\frac{\text{kg}}{\text{m}^3}\right]$

$$C_p = 4420{,}8 - 28{,}8x_{\text{ss}} + 2{,}4T \tag{7.8}$$

Where $C_p$ is the soursop's specific heat at constant pressure, $\left[\frac{\text{J}}{\text{kg°C}}\right]$

$$k = 0{,}605 - 5{,}3 \cdot 10^{-3}x_{\text{ss}} + 5{,}5 \cdot 10^{-4}T \tag{7.9}$$

Where $k$ is the soursop's thermal conductivity, $\left[\frac{\text{W}}{\text{m°C}}\right]$

Nonetheless, there is a general expression for viscosity for a power-law fluid which can be used in annular ducts, VM-Wärmeatlas [9] and Calculation procedure in CAS/P1 from Alfa Laval, Rolf Eklund. For non-Newtonian fluids, the viscosity is also known as the apparent viscosity [2].

$$\mu_{\text{app}} = KD^{n-1} \tag{7.10}$$

$$D = \frac{2\pi G}{AD_{\text{h}}\rho} \tag{7.11}$$

Where:

$K$ is the consistency index or power law coefficient,$\left[\frac{\text{kg}}{\text{ms}^{2-\text{n}}}\right]$
$n$ is the power law index, dimensionless
$G$ is the fluid mass flow rate, $\left[\frac{\text{kg}}{\text{s}}\right]$
$A$ is the cross-sectional area, [$\text{m}^2$]
$D_{\text{h}}$ is the hydraulic diameter, [m]

Once the physical properties have been defined, the Nusselt number correlation for the soursop juice under laminar flow for annular duct is the following [12].

$$\overline{Nu} = 6{,}41Gz^{\frac{1}{3}}\left(\frac{D_{\text{i}}}{D_{\text{o}}}\right)^{0{,}61} \tag{7.12}$$

Where $D_{\text{i}}$ is the external diameter of the inner cylinder and $D_{\text{o}}$ is the internal diameter of the outer cylinder for two coaxial cylinders. $Gz$ is the Graetz Number which is a non-dimensional number defined as it follows.

$$Gz = \frac{GC_p}{kL} \tag{7.13}$$

The friction factor correlations that were found for modeling the primary pressure drop for non-Newtonian fluids are described in Chapter 6. These correlations are the flat plates' correlation for non-Newtonian fluids following a power-law model, equation 6.14, and the soursop's juice correlation, equations 6.20 to 6.24. As it is

decided to work with the soursop's expressions, only the soursop's friction factor correlation will be used for the product side.

Water will be used as the utility medium. According to the results obtained previously, Monrad–Pelton's correlation will be used for calculating the Nusselt number in the heat transfer correlations as water usually runs under turbulent flow. In case the flow rate is very low reaching the laminar regime, the local Sieder–Tate Nusselt number correlation will be used. The friction factor will be calculated using Churchill's equation for both laminar and turbulent flows and the singular pressure drop coefficients are item's 11 factors, see Table 6.1.

The simulations performed in the code, once the previous modifications have been introduced, cover a Reynolds range for the product side from 1 to 200 resulting in 16 different cases. The water volumetric flow rate is set to be the double of the product flow rate. At the same time, a cooling and a heating case have been defined both covering the mentioned Reynolds range. When cooling, soursop at 40°C is cooled with water at 15°C and for the heating case, soursop at 15°C is heated with water at 40°C. For the soursop juice, according to [11] and [12], the content of soluble solids is set to be $x_{ss} = 25$°Brix, the consistency index $K$=32 $\left[\frac{kg}{ms^{2-n}}\right]$ and the power-law index $n$=0,32.

After performing the simulations, outgoing temperatures for the product and the utility side as well as pressure drops for both sides were obtained. Currently, these data are being evaluated with an Alfa Laval's program in order to be fit into a correlation.

# 8. Conclusions

A model considering both heat transfer and pressure drop has been modeled in this project for the ViscoLine Annular heat exchanger, a four concentric tubular heat exchanger from Alfa Laval AB. The VLA is a heat exchanger designed for dealing with non-Newtonian fluids. Although non-Newtonian fluids are common in our everyday life (food products like purees, chocolate, etc.), little research has been done in this field making the project substantially more difficult.

To obtain the model, a code in Pascal language has been developed in order to perform the heat transfer and pressure drop calculations. The validity of this code has been tested with the experimental data obtained from the laboratory tests. As it was not possible to perform the tests with non-Newtonian fluids and due to the lack of information regarding these fluids, tests were done using water and oil. Although tests were performed with different inserts, only one insert could be fully evaluated. For item 11 (product gap 9,8 mm) the heat transfer and the pressure drop model results showed very good results, less than 10% deviation.

Different Nusselt correlations were used to perform the heat transfer calculations depending on the type of flow regime. For the water/water test, water under turbulent flow, both Dittus–Boelter and Monrad–Pelton correlations presented the same results and almost the same values as the ones from the experimental test. For the oil/water test, for both cooling and heating cases, oil under laminar flow and water under turbulent flow, the combination of Sieder–Tate on the product side with either Monrad–Pelton or Dittus-Boelter on the utility side, showed the best results. However, when using the local Nusselt number, values presented a deviation of –25%. This deviation could be set to 0% if an empirical factor was introduced in Sider–Tate's local Nusselt number correlation. This factor should be approximately 1,5.

Different friction factor correlations were also used for calculating the primary pressure drops while the singular pressure drop coefficients were constant values obtained from literature. As well as for the heat transfer, different friction factor correlations were tested according to the flow regime. For the water/water test, the pressure drop results obtained for both product and utility were similar to the measured values. Furthermore, the best results were obtained with Churchill's and Swamee–Jain's correlations. For the oil/water test, the water side results were similar to those obtained in the water/water test. Nevertheless, in the product side, Churchill's and

$f = 16/Re$ were the correlations that presented best results although a difference between the cooling and the heating cases was observed. This difference could be due to the fact that the correlations do not consider a wall viscosity correction factor.

Furthermore, non-Newtonian data have been evaluated with the code and afterwards, the results have been used for obtaining the desired model for the VLA.

To summarize, the model obtained is reliable and thus, can be used for commercial purposes although there is still work to be done.

# 9. Improvements and Future Work

Most of the times you plan things the way you think are better to be done but once you have done them or while you are doing them, you realize that they could have been done in another way which would possibly give better results. In the following lines, improvements that have come up during this project are exposed. Besides, things you planned to last a given time usually last longer and thus, not everything you expected to cover could be achieved. Nevertheless, the most important points of this master thesis were covered although there is still work to be done in order to obtain a better model or confirm the present one.

### The Code

Regarding to the code elaboration, it may be possible to elaborate a code version that takes less time to perform the calculations although the current one works fast enough. Nevertheless, some code rearrangements can possibly be done. Besides, in the present code, specific data as tube diameters or the singular pressure drop coefficients ($\xi$ factors) which are dependent of the type of insert and the physical fluids'properties, are introduced as constant values as only data for two specific inserts were available. A practical improvement in the code if it is decided to work with it for commercial purposes, should be making the code able to read all these mentioned data from the files where they are stored. Hence, time would be saved as there would be no need for typing in all the possible diameters as well as all $\xi$ factors according to the different tube combinations. Furthermore, the program takes less space and to some extent, it is more practical.

### The Tests

Looking into how the tests were designed and run, it is obvious that other procedures are feasible as usually there is more than one way to do one thing. However, taking into account how it was done in this project, the oil/water tests should be studied more carefully. Therefore, when cooling or heating, the temperature difference the oil experienced was very small, around 1°C, which makes it harder to evaluate than if a larger temperature difference was possible. This means that a bigger temperature difference between the oil and the water should be used. However, things are not always as easy as they seem as oil or water cannot be always heated or cooled till a desired temperature without loosing the desired properties. Another thing that

should be done is to increase the Reynolds number in the heating oil case for item 11 to fully cover the laminar regime. Furthermore, an adiabatic test using oil/water as fluids should have been done to obtain pressure drop data without heat transfer.

### Data evaluation and CFD analysis

In Section 5.2, where the tests were described, it was mentioned that tests were run in the VLA using three different types of inserts: insert 11, insert 14 and insert 11 with static mixers. For both insert 11 and insert 14, water/water and oil/water tests were run and for item 11 with the static mixers only the water/water test as for technical reasons it was withdrawn from the project. However, due to the lack of time, only all item's 11 data from the test could be used to evaluate the generated code. Yet, the water/water test data from item 14 was evaluated showing good results for the heat transfer calculations but required some adjustments in the pressure drop calculations. This means that the pressure drop modeling should be studied more closely especially when changing inserts. Although there should not be any problem, results manifested that something was wrong. One must take into account that insert 14 was used in the usual item 11 unit which means that an extra expansion and contraction in the ears are present which could have a higher impact than expected so more work in this direction must be done. Moreover, all the oil/water test data for item 14 must be used to verify if the elaborated code is good enough or in order to improve it.

Item 11 with mixers was removed from the project for technical reasons. Despite the fact that the test data are available, these data cannot be used for further evaluations. Hence, new tests should be performed in an insert with static mixers as due to the type of fluids the VLA must deal with, static mixers are most of the times required in order to keep the homogeneity and the properties of the fluids like purees or other food products. It is very interesting to see and model the static mixers effect as they will produce an increase in the product pressure drop side which can be very important when designing the unit and setting the operation conditions. Thus, the incorporation of static mixers in the unit should be studied more closely, specially regarding pressure drop calculations.

Nonetheless, not all the data from the tests was used. This means that by evaluating these data, which are the temperatures at some point inside the VLA, not just the ingoing and outgoing temperatures, and the pressure drops between different parts of the unit, one could get a better idea of what happens in the inside of the VLA as it is not obvious due to the sudden expansions, contractions and different bends or other elements. This may help understand why the CFD analysis performed in the VLA provided worse results than those expected. Anyway, a closer look to the CFD analysis should be taken into consideration because by performing this technique, one should obtain closer results than those provided by constant values.

Yet, a CFD analysis allows you to obtain a correlation of the $\xi$ factor being function of a geometrical parameter, fact that would avoid having to calculate all the $\xi$ factors for all the elements for all the possible tube combinations and thus, save time.

### Wall viscosity effect

Furthermore, the wall viscosity correction factor for pressure drop calculations should be studied in more detail. No information regarding this topic was found in current literature although it is used for practical matters as referred in HTRI (Heat Transfer Research, Inc.). From the pressure drop results obtained for oil under laminar flow, a difference in results existed between the cooling and the heating cases which could possibly be because of the wall viscosity as a heated or cooled tube wall causes a gradient of physical properties between the wall and the fluid bulk distorting the velocity profile and thus affecting the pressure drop. Pressure drops results tended to improve when the use of the wall viscosity correction factor was simulated.

In general terms, more work must be done regarding pressure drop calculations by evaluating the existing and not used test data as well as continuing the initiated CFD analysis as mentioned in the previous chapter. Although heat transfer calculations seemed to give good results, the non-used data must be used in order to continue verifying the validity of the present model.

### New Design

Last but not least, the best improvement that could be done is redesigning the VLA. The actual design of the VLA is possibly not the best one that could be done. The main problem that presents this unit is all the bends and turns that it has. It is still not perfectly known what really happens inside the unit which makes it difficult to model, but taking into account that this heat exchanger is designed for viscous fluids, the less bends, the lower pressure drops, and moreover, bends or dead ends are perfect places for deposition or accumulation of solid particulates. Besides, almost all the bends, turns and the ears the VLA has are due to having the product in counter-current with the utility medium on both sides for higher heat transfer. Although a new design has not been modeled, some ideas are given in order to improve this unit. In order to still have the utility flowing in counter-current with the product but with less bends or other elements that interfere in the flow circulation, just a straight annular unit is possible but the fluid entrances and exits must be redesigned. In Figure 9.1 a sketch of a possible design is shown. As mentioned, it is possible to have a straight annular tube with the utility side flowing in counter-current as can be seen. Furthermore, with this design, pressure drops are much lower as no bends, turns, changes in section (from annular to circular or viceversa), elements that produce an obstruction to flow circulation, are present turning into a

stable flow profile. Due to its arrangement, tubes are easy to remove which facilitates its maintenance and cleaning operations and different units can be connected in series for industrial purposes. Nevertheless, calculations should be done to verify the viability of this possible new model.

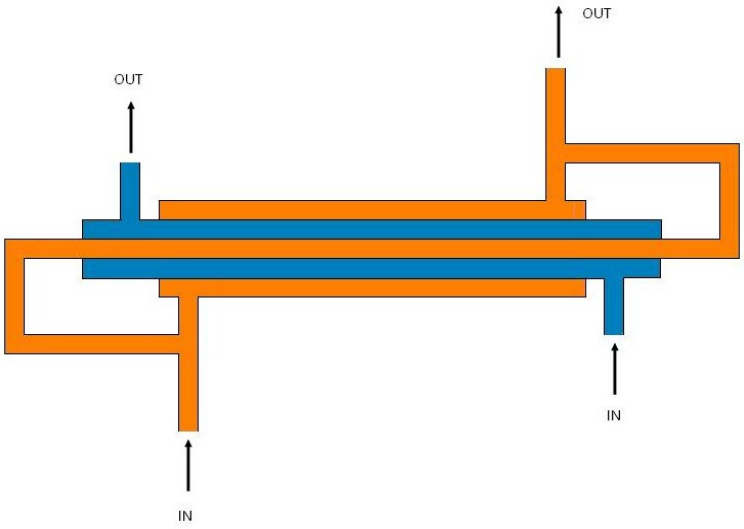


Figure 9.1: Sketch of a possible VLA design

# 10. Acknowledgments

First of all I would like to thank my supervisor PhD Henrik Kockum for his continuous support, encouragement, patience and help during these months.

I would also like to thank Martin Johansson for the project as without him this could not have been possible. Thank you as well for answering all the technical questions and for supplying the units for the test.

Lots of thanks also to Martin Holm for dedicating some of his time to perform the CFD analysis on the unit and to Anders Dahl and Milos Milovancevic for all the work done in the Test Center: setting the unit for the tests, performing the tests, etc. and for answering all my questions and doubts.

Special thanks to Professor Ulf Bolmstedt for helping, sharing and guiding me through the literature research as well for the useful conversations and given advices.

A special thank to the staff of the Thermal Design Department and the other master thesis students for the interesting and helpful discussions during meetings, lunches, *fika* times as well as for helping me feel like being home and improve my Swedish.

Last, infinite thanks to my parents, Miquel and Neus, and my brother Albert. Thanks for all the support you have given me throughout all these years and for being there even the distance. Sense el vostre continu suport i la vostra infinita paciència res no hagués sigut possible.

# Bibliography


[1] ViscoLine Annular Unit, The tubular heat exchanger series from Alfa Laval, brochure.

[2] Perry, Robert H; Green, Don W. *Perry's Chemical Engineers'Handbook.* 7th ed. McGraw-Hill, 1999.

[3] Idelchik, I.E. *Handbook of Hydraulic Resistance.* 3rd ed. Begell House, 1996.

[4] Incropera, Frank P; De Witt, David P. *Fundamentos de Transferencia de Calor.* 4th ed. México: Prentice Hall, 1999.

[5] Chhabra, R.P; Richardson, J.F. *Non-Newtonian Flow and Applied Rheology: Engineering Applications.* 2nd ed. Elsevier, 2008.

[6] Byron Bird, R.; Stewart, Warren E.; Lightfoot, Edwin N. *Tranport Phenomena.* Wisconsin: John Wiley and sons, 1960.

[7] Calleja Pardo, G; García Herruzo, F; de Lucas Martínez, A; Prats Rico, D; Rodríguez Maroto, JM. *Introducción a la Ingeniería Química.* 1st ed. Madrid: Sintesis, 1999.

[8] McCabe, Warren L.; Smith, Julian C.; Harriot, Peter. *Unit Operations of Chemical Engineering.* 7th ed. New York: McGRaw Hill, 2004.

[9] *VDI-WÄRMEATLAS.* 3rd ed. Düsseldorf: VDI-verlag GmbH, 1977.

[10] Kockum, Henrik. *Aspects of Sorption Processes in Thermosiphon and in Falling Film Arrangements.*PhD Dissertation. Lund, Sweden: Department of Chemical Engineering, Lund University, September 1998.

[11] Gratão, A.C.A; Silveira Jr, V; Telis-Romero, J. "Laminar flow of soursop juice trough concentric annuli: Friction factors and rheology". *Journal of Food Engineering*, $n°78$ (2007), p.1343−1354.

[12] Gratão, A.C.A; Silveira Jr, V; Telis-Romero, J. "Laminar forced convection to a pseudoplastic fluid food in circular and annular ducts". *International Communications in Heat and Mass Transfern°*33 (2006), p.451−457.

[13] Andersson, Matz. "Generell härledning av friktionskoefficienten". *Teori om tryckfall i kanaler, Alfa Laval Lund: PC CHE TD* , (2007), p.1−9.

[14] Churchill, S.W. "Friction-factor Equation Spans All Fluid-flow Regimes". *Chemical Engineering*, $n°$**84**(24) (1977), p.91−92).

[15] Trillas Gay, Enrique. *Circulació de Fluids, notes from the course.* Barcelona: Escola Tècnica Superior d'Enginyeria Industrial de Barcelona, 2008.

[16] Velo, Enrique. *Disseny d'Equips Tèrmics 1: Convecció, notes from the course.* Barcelona: Escola Tècnica Superior d'Enginyeria Industrial de Barcelona, February 2009.

[17] Dahl, Anders. "General Test Procedure for determining the thermal and/or hydraulic performance of heat exchangers". *Test Procedures, Alfa Laval lund: PC CHE*, (March 2010), p.1−6.

[18] AVD för Kemisk Apparatteknik. *Formelsamling: Strömningsteknik och Värmeteknik.* Lund: Lunds Tekniska Högskola (LTH), 1988-1989.

[19] Nuclear Power Fundamentals. *Flow Velocity Profiles* [online].< *http* : *//www.tpub.com/content/doe/h*1012*v*3*/css/h*1012*v*3$_4$0*.htm* > [17/10/2010].